A *Gnl1*-dependent Natural Killer cell deficiency is associated with altered cell cycle and ribosomal protein gene expression and is overcome by p53 ablation

By

Natasha Barone

Department of Microbiology & Immunology

McGill University, Montreal, Quebec, Canada

April 2019

A thesis submitted to McGill University in partial fulfillment of the requirements of the degree of Master of Science.

Abstract

Natural Killer (NK) cells are the founding members of the innate lymphoid cell family. They are bone marrow derived effector lymphocytes that have cytotoxic and regulatory capacities which provide protection against viral infection and tumor formation. Following an *N*-ethyl-*N*-nitrosourea (ENU) induced mutagenesis screen in mice, we identified a pedigree with severe susceptibility to murine cytomegalovirus (MCMV) infection due to a loss-of-function mutation in the gene, *Guanine nucleotide-binding protein-like 1* (*Gnl1*). The mutation introduces a premature stop codon at amino acid position 365 (mutant = $Gnl1^{C365X}$), resulting in an NK cell deficiency.

The **overall objective** of this study is to understand the mechanism by which mutation of GNL1 leads to NK cell deficiency. Based on the close sequence homology of GNL1 to other YRG family proteins and reports on the function of human GNL1, we **hypothesize** that the $Gnl1^{C365X}$ mutation perturbs ribosomal protein and cell cycle gene expression, p53 activation and cell survival in NK cells.

In order to address the hypothesis, we performed RNA-sequencing to identify differentially expressed genes (DEGs) between $Gnl1^{+/+}$ and $Gnl1^{C365X}$ NK cells. A total of 143 DEGs were identified. Gene ontology highlighted terms associated with cell cycle, and cell cycle checkpoints. A gene set enrichment analysis (GSEA) using immunological or KEGG gene sets demonstrated a positive enrichment in cell cycle and a negative enrichment in ribosome signatures in $Gnl1^{C365X}$ NK cells. *Bub1*, *Bub1b* and *Plk1* were three cell cycle genes among the 143 DEGs leading the enrichment of the KEGG cell cycle pathway. *Bub1*, *Bub1b* and *Plk1* contain p53 responsive elements and have been shown to interact with p53. Ribosomal transcripts were reduced in the $Gnl1^{C365X}$ NK cells which could be inducing ribosomal stress to activate p53 pathways.

By knocking out the cell fate gate keeper p53, we were able to rescue the MCMV susceptibility observed in $Gnl1^{C365X}$ mice. Moreover, the $Gnl1^{C365X}$ NK cell deficiency, caspase 3 levels, and receptor expression (KLRG1, NKG2D, Ly49H, Ly49G2 and CD122) were restored to wild-type levels. In this study, we highlight that $Gnl1^{C365X}$ NK cells are undergoing p53-dependent apoptotic cell death and the NK cell deficiency is underlying the susceptibility to MCMV infection. Furthermore, our data suggests that a downregulation in ribosomal protein transcription induces p53 activation resulting in abnormal NK cell cycle, proliferation and survival.

Résumé

Les cellules de type NK sont les membres fondateurs de la famille des cellules lymphoïdes innées. Elles sont regroupées auprès des lymphocytes effecteurs formés dans la moelle osseuse, mais se distinguent par leurs capacités cytotoxiques et régulatrices qui leur permettent de combattre les infections virales et d'empêcher la formation de tumeurs. En utilisant une plateforme de mutagenèse *N*-ethyl-*N*-nitrosourea (ENU) chez la souris, nous avons identifié une mutation dans le gène *Guanine nucleotide-binding protein-like 1 (Gnl1)* entraînant une perte de fonction et menant à la susceptibilité à l'infection au cytomégalovirus murin (MCMV). La mutation introduit de façon prématurée un codon-stop à la position 365 de la séquence d'acide aminée de *Gnl1* (mutant = $Gnl1^{C365X}$), ce qui provoque une déficience dans les cellules de types NK.

L'objectif général de cette étude est de comprendre le mécanisme par lequel la mutation de *Gnl1* pourrait conduire à une déficience en cellules NK. En tenant compte de la très forte homologie entre *Gnl1* et les autres membres de la famille de protéine YRG, et des quelques études ayant établies des fonctions moléculaires pour le gène GNL1 humain, nous formulons l'hypothèse que dans les cellules NK, la mutation $Gnl1^{C365X}$ perturbe l'expression de gènes ribosomaux, l'expression de gènes liés au cycle cellulaire, l'activation de p53, et la survie cellulaire.

Afin de vérifier cette hypothèse, l'emploie du séquençage de l'ARN nous a permis d'identifier un total de 143 gènes exprimés de façon différentielle entre les cellules NK $Gnl1^{+/+}$ et $Gnl1^{C365X}$. Une analyse « Gene Ontology » nous a d'abord permis de regrouper ces gènes par catégories fonctionnelles, et de constater que de nombreux gènes étaient étroitement liés au contrôle et au fonctionnement du cycle cellulaire. Au nombre de ces gènes exprimés, nous avons évaluer à l'aide d'une analyse GSEA la représentation de divers ensembles de gènes appartenant à des voies moléculaire (KEGG) ou à des voies immunitaires, et avons identifié, auprès des cellules NK $Gnl1^{C365X}$, la surreprésentation de fonctions liées au cycle cellulaire, et la sous-représentation de fonctions ribosomales. Parmi nos gènes exprimés différemment, les gènes *Bub1*, *Bub1b* et *Plk1* se sont démarqués par leur rôle au sein des voies p53. D'autre part, de nombreux transcrits d'ARN de protéines ribosomiales étaient réduits dans les cellules NK mutantes, ce qui pourraient promouvoir l'activation de voies p53.

Par conséquent, l'élimination de p53 par « knock-out » nous a permis de surmonter la susceptibilité des souris $Gnl1^{C365X}$ face au virus MCMV, en plus de corriger la déficience en

cellules NK, les niveaux d'expression de caspase 3 et l'expression de récepteurs NK (KLRG1, NKG2D, Ly49H, Ly49G2 and CD122), pour rejoindre l'état normal des souris *Gnl1*$^{+/+}$.

Dans la présente étude, nous démontrons que les cellules NK *Gnl1*^{C365X} sont plus vulnérables à la mort cellulaire par les voies p53 et celle de l'apoptose, ce qui contribue à une déficience en cellules NK et entraîne une susceptibilité à l'infection MCMV. De plus, nous suggérons qu'une transcription diminuée de gènes ribosomaux, et l'activation subséquente de p53, pourrait mener à de profonds défauts au niveau de l'induction du cycle cellulaire, de la prolifération des cellules NK, et de leur survie.

Table of contents

Abstract…… 2
Résumé…… 3
Table of contents…… 5
Acknowledgements…… 7
List of Abbreviations…… 8
List of Figures and Tables …… 10
Author contributions…… 11
Chapter 1: Introduction & Literature Review…… 12
1.1 NK cell identity, development and maturation…… 12
1.1.1 NK cell discovery…… 12
1.1.2 Cell surface phenotype for identifying NK cells …… 12
1.1.3 NK cell development…… 12
1.1.4 NK cell maturation…… 14
1.1.5 NK cells as ILCs…… 15
1.1.6 NK cell sub-types…… 15
1.2 Regulation of NK cell activity…… 16
1.2.1 Target cell recognition…… 16
1.2.2 NK cell receptors…… 16
1.2.3 Signaling pathway of NK cell receptors…… 18
1.2.4 NK cell education…… 19
1.2.5 NK cell regulation by inflammatory cytokines and cross-talk with DCs and Neutrophils…… 19
1.2.6 NK cell regulation by homeostatic IL-2/IL-15 cytokines…… 20
1.2.7 Signaling pathways downstream of IL-2/IL-15…… 21
1.3 NK cell responses…… 23
1.3.1 Cytotoxicity…… 23
1.3.2 Cytokine secretion…… 24
1.3.3 NK cell memory…… 24
1.4 The mouse model of cytomegalovirus infection to understand NK cell biology…… 26
1.4.1 Cytomegalovirus…… 26

1.4.2 *Gnl1*^{C365X} mutation results in an NK cell deficiency…….. 27
1.5 The GNL1 gene family…….. 28
Chapter 2: Rationale & Objectives…… 30
2.1 Rationale and hypothesis…… 30
2.2 Objectives and aims……... 30
Chapter 3: Materials & Methods……... 31
Chapter 4: Results……... 36
4.1 *Gnl1*^{C365X} NK cells undergo increased apoptotic cell death……..... 36
4.2 GNL1-dependent pathways in NK cells…….. 38
4.3 Gene ontology on 143 DEGs highlights differences in cell cycle processes…….. 38
4.4 GSEA analysis identifies cell cycle and ribosome signatures...…...…….. 41
4.5 *Gnl1*^{C365X} NK cells have increased susceptibility to p53-dependent cell death…..…. 46
4.6 Knock out of *Trp53* rescues MCMV susceptibility and NK cell deficiency…….. 48
4.7 *Trp53* KO restores NK cell maturation and receptor expression…… 50
Chapter 5: Discussion…… 52
Chapter 6: Final conclusions & summary…… 58
References…… 59
Appendix……71

Acknowledgements

First, I would like to thank Dr. Silvia Vidal for having given me the opportunity to be a member of her laboratory and for allowing me to work on the GNL1 project. She was a great mentor and helped me become both a better scientist and individual and for that I will be forever grateful. I would also like to thank her for pushing me not to give up on my goals and to see that there is always a solution. Lastly, I would like to thank her for editing this thesis.

I would like to thank my committee members Dr. Martin Richer and Dr. Anastasia Nijnik for providing guidance throughout the entire project and for putting me in contact with their students to learn techniques which enabled my project to move forward.

Many thanks to my current and past lab members - Benoit Charbonneau (my favorite support staff), thank you for making me laugh each day even when times were hard. I owe you many 5$ bucks (haha!). Salma Chehboun – thank you for coming in at 5am with me repeatedly to run experiments (I know how much you love your sleep). You are a dear friend to me, and I will always remember our celebratory morning coffees. Mathieu Mancini – Thank you for brainstorming with me since the very beginning and being a great mentor, you have made me a better scientist. Also, many thanks for editing my French abstract and the RNA-sequencing figure legends.

I would also like to thank my family and my boyfriend Matthew Mannarino for being a great support system. I must have presented my presentation to you all at least 100x within the last year – thank you for not giving up on me and dealing with my craziness! Also, thanks Matt for brainstorming with me and staying on the phone all those nights when I was writing up class projects. I will never forget the all-nighter we did the night before I submitted the thesis. Famiglia et amore mio, ti amo con tutto il mio cuore.

List of Abbreviations

Act D	Actinomycin D
APC	Antigen Presenting Cell
B10	C57BL/10
B6	C57BL/6
BM	Bone marrow
CILP	Common innate lymphoid progenitor
CLP	Common lymphoid progenitor
CMP	Common myeloid progenitor
CMV	Cytomegalovirus
cNK	Conventional Natural Killer cell
DC	Dendritic cell
DEG	Differentially expressed gene
DN	Double negative
DP	Double positive
EILP	Early innate lymphoid progenitor
ENU	*N*-ethyl-*N*-nitrosourea
GMP	Granulocyte/macrophage progenitors
Gnl1/GNL1	Guanine Nucleotide Binding Protein Like 1
GO	Gene ontology
GSEA	Gene set enrichment analysis
HSC	Hematopoietic Stem Cell
i.v.	Intravenous
IFN	Interferon
IL	Interleukin
IL-2R	Interleukin-2 receptor
IL-5R	Interleukin-5 receptor
ILC	Innate lymphoid cell
iNK	Immature natural killer
KO	Knock out
LT	Long term
MCMV	Murine cytomegalovirus
MEP	Megakaryocyte/Erythrocyte progenitor
MHC-I	Major Histocompatibility complex I
mNK	Mature natural killer
MPP	Multipotent progenitor
mTOR	Metabolic target of rapamycin
NK	Natural killer
NKar	Natural Killer activity receptor
NKir	Natural Killer inhibitory receptor

NKP	Natural Killer cell precursor
Pre-NKP	Pre-natural killer cell precursor
RBC	Red blood cell
SP	Single positive
ST	Short term
STAT	Signal transducer and activators of transcription
TF	Transcription Factor
Th1	Type 1 T helper
trNK	Tissue resident NK cell

List of Figures & Tables

Chapter 1: Introduction & Literature Review

Fig. 1: Cellular stages of NK cell development……14

Fig. 2: IL-15 signaling pathways in NK cells……. 23

Chapter 4: Results

Fig. 3: *Gnl1*^{C365X} NK cells undergo increased apoptotic cell death …… 37

Fig. 4: *Gnl1*^{C365X} NK cells differentially express 143 genes ……..……. 40

Fig. 5: Cell cycle genes are leading the enrichment of immunological signatures in *Gnl1*^{C365X} NK cells…….…….. 42

Fig. 6: Altered cell cycle and ribosomal protein gene expression in the KEGG pathway.....… 45

Fig. 7: Actinomycin D further promotes *Gnl1*^{C365X} NK cell death via p53 ……...…. 47

Fig. 8: *Trp53* KO overcomes MCMV susceptibility and NK cell deficiency while restoring normal caspase 3 expression in *Gnl1*^{C365X} NK cells…….……..... 49

Fig. 9: *Trp53* KO in *Gnl1*^{C365X} mice restores NK cell maturational program and receptor expression…..…… 51

Chapter 5:

Fig. 10: Working model…… 56

Appendix

Table A1: Flow cytometry antibodies…….…. 71

Table A2: Cell sorting antibody panel…….…. 71

Table A3: NK cell purity and RNA quality…….……..… 72

Table A4: RNA-sequencing set-up and quality control…….……... 72

Table A5: Sequencing alignment results…….…….. 72

Fig. A1: Flow cytometry gating strategies…….…….73

Fig. A2 - NK cell sorting gating strategy…….…..74

Author contributions

Chapter 1 – Introduction & Literature Review

The introduction and literature review were written by NB and edited by SV.

Chapter 2 – Rationale & objectives

The rationale and objectives were written by NB and edited by SV.

Chapter 3 – Materials & Methods

The materials and methods were written by NB and edited by SV

Chapter 4 – Results

Barone, N., Chehboun, S., Mancini, M., Charbonneau, B., Leiva, G., D'Arcy, P., Vidal., S.

Chapter 4 was written by NB and edited by SV. NB performed mouse experiments for flow cytometry with assistance from SC. Sorting protocol was developed by NB. SC aided in the preparation of samples for sorting. Camille Stegen and Julien Leconte from the flow cytometry core sorted the samples. Dr. Odile Neyret and Myriam Rondeau from the molecular biology platform at the IRCM confirmed RNA quality, prepared the cDNA library and performed RNA sequencing. José Hector Lopéz from the Canadian Centre of Computational Genomics (C3G) ran the RNA-sequencing pipeline on the data; from trimming step up to and including EdgeR/Deseq2 packages. NB selected fold change and p-value cut-offs produced volcano plots and performed visualization using IGV and performed Gene ontology. MM performed the GSEA and prepared the associated visuals. BC identified the Glynn pedigree using the MCMV screen and performed genotyping on all the mice. GL identified the *Gnl1* mutation, the NK cell deficiency and associated phenotypes of $Gnl1^{C365X}$ mice and performed preliminary studies in $Gnl1^{C365X}Trp53^{-/-}$ mice. Mice used in the MCMV infection were infected by PD and were monitored by SC. All breeding and maintenance of the colony was done by PD.

Chapter 5 – Discussion

The discussion was written by NB and edited by SV.

Chapter 6 – Final conclusions & summary

The final conclusions and summary were written by NB and edited by SV.

Chapter 1 – Introduction & Literature Review

1.1 NK cell identity, development and maturation

1.1.1 NK cell discovery

In 1970, it was believed that the only two categories of lymphocytes that existed were T or B cells and therefore, much of the research was focused on characterizing these cell types (1). While studying T cell-mediated cytotoxicity, investigators identified a subset of large agranular lymphocytes originating from the bone marrow (BM) which were not T or B cells (2). Over a period of 5 years, researchers identified that these cells were cytotoxic and had the remarkable capacity to kill tumor cells without prior sensitization (1). Based on these features, Rolf Keissling termed these cells Natural Killer (NK) cells in 1975 (1). Since then, a significant amount of research has been focused on identifying the role of these cells. Today, it is known that NK cells are members of the family of innate lymphoid cells. Furthermore, NK cells distinguish themselves as effector lymphocytes of the innate immune system endowed with both cytotoxic and regulatory capacities that provide anti-tumor and anti-viral responses (3).

1.1.2 Cell surface phenotype for identifying NK cells

In humans, NK cells are identified based on the expression of the surface markers $CD56^{+}$ $CD3^{-}$ and more recently $NKp46^{+}$ (4). They are further divided into $CD56^{bright}$ and $CD56^{dim}$ NK cells. While in C57BL/6 mice, NK cells are identified by the presence of $NK1.1^{+}$ (NKR-P1C), $NKp46^{+}$ (NCR1), $CD49b^{+}$ (DX5) surface receptors and the absence of CD3 expression (2, 4).

1.1.3 NK cell development

In order for an NK cell to develop, a cell differentiation process must occur. At the origin of hematopoiesis; production of all the cells of the blood, are the multipotent hematopoietic stem cells (HSCs) (5). In mice, hematopoietic activity begins in the yolk sac. Cells can then undergo extensive cell division in the fetal liver prior to being shuttled through the blood to the BM and other tissues (6). In the BM, HSCs develop into long-term (LT) HSC progenitors which can then give rise to short-term (ST) HSCs (7, 8). ST HSCs further differentiate into multipotent progenitors (MPPs) (5, 7, 9). MPPs can either differentiate into common myeloid progenitors (CMP) or common lymphoid progenitors (CLP) (5, 10, 11). CMPs further differentiate into the megakaryocyte/erythrocyte progenitor (MEPs) or into granulocyte/macrophage progenitors

(GMPs) (5). CLPs give rise to all lymphocytes, including small lymphocytes such as T cells, B cells or large granular lymphocytes such as NK cells and other ILCs (5). A definite model regarding NK cell development remains to be determined (12). At this point, the earliest lineage resulting in NK/ILCs is the early innate lymphoid progenitor (EILP) (13). The common innate lymphoid (CILP/αLP) progenitor has also been identified; it develops from the CLPs to give rise to all ILCs (14). The relationship between EILPs and CILPs has yet to be characterized, however, it is known that the CILP gives origin to the pre-NK precursor (pre-NKP/pre-proNKP) (15). The pre-NKP cells then develops into NK cell precursors (NKP) cells which then become immature NK cells (iNK) that develop into mature NK (mNK) cells (16). Mature NK cells exit the BM and re-circulate in the blood to survey the environment and respond to viruses and tumors (15, 17). Transcription factors (TFs) regulating the developmental program as well as the typical surface markers for each population are shown in Figure 1.

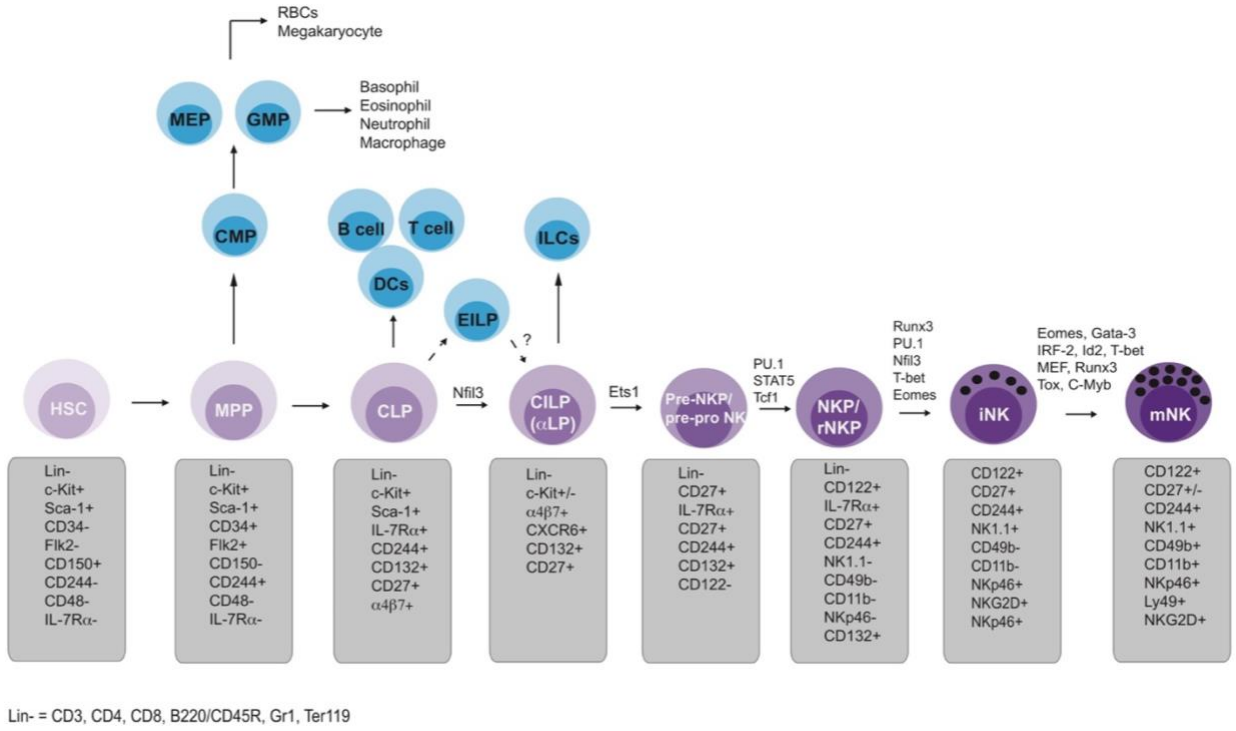

Figure 1: Cellular stages of NK cell development
NK cell development in the mouse BM requires a diverse profile of transcription factors. Surface markers used to identify each population stemming back to the HSCs is shown and based predominantly from (12, 18) but also inspired from (19-21).Developmental order and TFs presented are based and inspired by figures and studies discussed/shown in (5, 12, 13, 15, 16, 18, 22). TFs positions are shown based on where earliest effect has been reported, however it is known that the TFs can be present at different concentrations throughout the developmental process.

1.1.4 NK cell maturation

The presence of a fully functional and mature (m)NK cell compartment is crucial for proper expression and NK cell effector functions against viral infections and tumor formation (23). mNK cells are not uniform; once NK cells reach the final stage in NK cell development and become mNKs, they undergo a maturation program consisting of 4 stages which depend on the differential expression of CD27 and CD11b (Mac-1) in mice (23). These populations are the double negative (DN), CD27 single positive (SP), double positive (DP) and the CD11b SP NK cell populations; whereby the DN are the least mature mNKs and CD11b SP NK cells are the most mature mNKs. In studies performed on other lymphocytes, maturation programs have been associated with

different functions. In NK cells, it was identified that the maturation program was associated with proliferative capacity and effector function. More specifically, the less mature CD27 SP mNKs were found to have a higher proliferative capacity and the most mature CD11b SP mNK cells were found to have the highest effector (cytotoxic) potential (23). Moreover, the CD27 SP mNK cells were found to be enriched for transcripts encoding cyclin, cyclin dependent kinase genes, chromosome condensation and microtubule-based movement proteins; all proteins associated with cell cycle when compared to the more mature CD11b SP mNKs (23).

1.1.5 NK cells as ILCs

In terms of frequency, NK cells are one of the three major lymphocyte populations which are further classified as innate lymphoid cells (ILCs) (24, 25). By analogy with T helper cells, ILCs are divided into four groups according to differential effector cytokine expression and developmental requirement for transcription factors: ILC1; ILC2; ILC3, which includes ILC3s and lymphoid tissue inducer (LTi) cells; and ILC4 (25, 26). Key characteristics of ILCs include; (i) ILCs have a lymphoid morphology. (ii) ILCs do not undergo Rag-dependent rearrangement of antigen receptors and (iii) ILCs lack myeloid phenotypic markers (25). Group 1 ILCs consist of NK cells and ILC1s which are capable of producing IFN-γ and TNF-α and depend on the transcription factor T-bet for their development (25, 26). However only NK cells require EOMES while ILC1s do not (25, 26). Moreover, unlike ILC1s, NK cells are cytotoxic (2). Group 2 ILCs include ILC2s which secrete IL-5, IL-13, IL-6 and IL-9 and they require GATA-3 for their development (25, 26). Group 3 ILCs include ILC3s and LTis which secrete IL-17 and/or IL-22 and depend on the transcription factor RORγT for development (25, 26). The ILC4 group include NK17/NK1 cells which produce IFN-γ and IL-17 and depend on TFs RORγT and T-bet during development (25, 26). ILCs have been suggested to act as the innate counterpart of adaptive immune cells. For example, Group 1 ILCs have transcription/cytokine profiles similar to those found in a type 1 immune response while Group 2 ILCs are more similar to type 2 responses (25). Group 3 ILCs are similar to Th17/Th22 cells (25, 26).

1.1.6 NK cell sub-types

NK cells are distributed in many tissues/organs of the body including the BM, spleen, peripheral blood, liver, thymus, lymph node, uterus and the skin (27, 28). Two categories of NK cells that exist include conventional/circulatory NK (cNK) cells and tissue-resident NK (trNK)

cells. The main site of NK cell development is the BM (29). NK cells which follow traditional development/maturation/education begin in the BM and then migrate towards different sites for both homeostatic immune surveillance and in response to infection/invasion. However, NK cells can develop in the fetal liver or the thymus (30). Liver NK cells originate when HSCs migrate to the fetal liver during embryonic development and remain there instead of migrating and colonizing the BM (31). Two distinct NK cell subsets can be identified in the liver based on the differential expression of CD49a and CD49b; $CD49a^{+}CD49b^{-}$ and $CD49a^{-}CD49b^{+}$ (28). $CD49a^{+}CD49b^{-}$ are liver-resident NK cells (trNKs) while $CD49a^{-}CD49b^{+}$ are cNK cells (28). $CD49a^{+}CD49b^{-}$ express high levels of the cytotoxic molecule TRAIL ($TRAIL^{+}$) (28). Recently, it was found that $CD49a^{+}CD49b^{-}$ staining can also be used to identify trNK cells in the uterus and skin (28, 32). Thymic NK cells originate from pro-T progenitors which migrate from the bone marrow to the thymus; they are characterized by the expression of CD127 (IL-7Rα) and GATA-3 and (29, 33).

1.2 Regulation of NK cell activity

1.2.1 Target cell recognition

NK cells unlike other immune cells do not require prior immunization to function (34-36). Rather, they receive activating and inhibitory signals via the interaction of their activating (NKar) and inhibitory (NKir) receptors with cellular stress ligands, major histocompatibility complex 1 (MHC-I) or MHC-I like molecules which allow them to determine whether they will initiate target cell killing (37). Healthy cells express a high level of MHC-I which can bind to NKirs of NK cells thereby inducing self-recognition and inhibiting NK cell activation and killing from occurring (38). However, virus-infected and/or tumor cells (target cells) downregulate the expression of MHC-I on their surface which results in a killing signal to be induced (missing-self hypothesis) (38, 39). The missing self-hypothesis was further proven by the fact that in the absence the light chain of MHC-I (β2m) which is required for MHC-I surface expression was removed, cells became susceptible to NK cell killing (39, 40).

1.2.2 NK cell receptors

The major role of NK cells is to provide efficient anti-tumor and anti-viral responses. In order to do so, NK cells must express a variety of receptors. One receptor family that NK cells

express in both mice and humans is the activating natural cytotoxicity receptor (NCR) family (41). This family consists of NKp46 (NCR1/CD335), NKp44 (NCR2, CD336) and NKp30 (NCR3, CD337) (41). Humans express all three receptors while mouse NK cells only express NKp46 (42). These receptors are able to recognize both virally infected and tumorigenic cells (41). Both NKp46 and NKp44 can recognize influenza virus and Sendai virus (41, 43). Recognition/killing of target cells infected with influenza virus or Sendai virus is initiated upon binding of viral proteins. NKp44 binds the viral protein hemagglutinin of either influenza virus or Sendai virus to recognize the viruses while NKp46 binds the hemagglutinin of influenza virus or the hemagluttinin-neuraminadase of Sendai virus to initiate target cell killing (41). Interestingly, human NK cells can induce neutrophil apoptosis via a NKp46-/Fas-dependent mechanism (44).

As previously mentioned, mouse NK cells express Ly49 family of receptors which can be activating or inhibitory (39). They are homodimeric type II glycoproteins of the C-type lectin superfamily (39). mNK cells can randomly express one or more of these receptors (45). In mice, the genes encoding the Ly49 family are found in the natural killer gene complex (NKC) on chromosome 6 (41). Ly49H and Ly49D are NKars while Ly49A, C, E, F, G, I, J and Q are inhibitory (39). Inhibitory Ly49s are generally characterized for their role in NK cell education and preventing autoimmunity while the activating receptors promote NK cell cytotoxicity and cytokine production (39). Ly49H (NKar) directly interacts with the m157 protein of mouse cytomegalovirus to provide resistance against MCMV (46). This is further illustrated by the fact that 129 and BALB/c mice which lack Ly49H are highly susceptible to MCMV infection (39). Human NK cells do not express Ly49 receptor genes but express KIR genes and receptors which are located in the Leucocyte Receptor Complex (LRC) on chromosome 19q13.4 (47, 48). They are the major receptors recognizing MHC-I in NK cells. Activating KIRS found on human NK cells include; KIR2DL4, KIR2DS1, KIR2DS2, KIR2DS3, KIR2DS4, KIR2DS5 and KIR3DS1 (39). Inhibitory KIRs found on NK cells include KIR2DL1, KIR2DL2, KIR2DL3, KIR2DL5, KIR3DL1 and KIR3DL2 (39).

NK cells also express the C-type lectin receptor CD94 in combination with NKG2A/C/E. NKG2A/CD94 can bind MHC-I molecule Qa-1^b in mice or HLA-E in humans on target cells to prevent activation (49). This occurs using immunoreceptor tyrosine-based inhibition motif (ITIM) signaling via ITIMs in the cytoplasmic tail of NKG2A (50). CD94 can also interact with NKG2C/E

to activate NK cell signalling (48, 51). NKG2D is a type II transmembrane glycoprotein with a C-type lectin-like domain (52). It does not interact with CD94 and has a low sequence homology to NKG2A/C/E (48). NKG2D can bind a variety of ligands to promote its activation in both humans and mice (52). In mice, it can bind Rae-1 like proteins and H-60 (51). NKG2D is important for control of MCMV/HCMV infections and many tumor types (52, 53). NKG2, NKG2A/C/E as well as NKG2D are all found within the NKC of mice and humans (48).

Two other important receptors are CD69 and KLRG1. The C-type lectin CD69, also referred to as the very early activation antigen is not expressed on resting NK cells but is upregulated following NK cell activation (54, 55). The killer cell lectin-like receptor G1 (KLRG1) is a C-type lectin which contains an ITIM in its cytoplasmic domain and is found on 30-40% resting NK cells (54, 56). It is a marker of terminal maturation in NK cells (2). KLRG1 can bind to E-, N- and R- cadherin (57). Since KLRG1 is expressed on phenotypically mature NK cells, it can also be used as a marker to identify this NK cell population (58). NK cells expressing KLRG1 are less proliferative in response to IL-15, secrete reduced levels of IFN-γ and undergo increased apoptotic cell death (57, 59, 60). Following MCMV infection, a large expansion of $KLRG1^+$ cells occurs; however, these cells undergo apoptosis during NK cell contraction (54, 60, 61).

1.2.3 Signalling pathway of NK cell receptors

In their cytoplasmic tail, inhibitory receptors involved in target cell recognition have immunoreceptor tyrosine-based inhibitory motifs (ITIMs) (48). Activating receptors either have the immunoreceptor tyrosine-based activation motifs (ITAMs) in their cytoplasmic tail or can non-covalently associate with adaptor proteins such as DAP10, DAP12 to provide activating signals (62). ITAMs are the antagonists of ITIMS and vice-versa. Following antigen-inhibitory receptor binding in NK cells, the ITIM becomes phosphorylated on its tyrosine residues (39). Once phosphorylated it can recruit the src homology 2 (SH2) domain containing tyrosine phosphatases SHP-1 and SHP-2 which can inhibit activating signals to prevent killing of normal cells expressing MHC-I (39). However, when the activating receptors bind antigens, ITAMs can become phosphorylated to recruit Syk and Zap70 via their SH2 domains which promotes NK cell cytotoxic degranulation and transcription of cytokine/chemokine genes to kill target cells (62).

1.2.4 NK cell education

NK cell receptor-ligand interactions mediate a process essential for NK cells to attain functional maturation and self-tolerance: NK cell education. Three main forms of education have been reported which include; (a) classical NK cell education (licensing), (b) non-classical MHC-I dependent NK cell education, (c) MHC-I independent NK cell education.

(a) NK cell activation is mainly regulated by interactions with self MHC-I molecules. The best characterized receptors that specifically bind MHC-I molecules are the inhibitory Ly49s in mice and KIRs in humans (Killer cell immunoglobulin like receptors) (63). Only NK cells whose inhibitory receptors have been engaged will be fully competent; this process is termed classical NK cell education or NK cell licensing (63). This has been highlighted by the fact that MHC-I deficient mice and Ly49 deficient mice poorly reject target cells lacking MHC-I expression (63-65). Licensed NK cells can efficiently recognize target cells void of MHC-I and do not target MHC-I hosts (63). However, unlicensed NK cells are hypo-responsive; they cannot recognize missing MHC-I target cells and they can attack MHC-I expressing cells (63).

(b, c) Aside from the classical inhibitory Ly49s and KIRs, other inhibitory MHC-I specific receptors can be used to educate NK cells. Non-classical MHC-I dependent education can occur when MHC-Ib (HLA-E in humans, Qa-1 in mice) interacts the inhibitory receptor CD94/NKG2A (49, 63). Moreover, MHC-I independent NK cell education can occur. For example, 2B4 receptors bind the CD48 ligand to promote NK cell education; 2B4 and CD48 knock out mice were incapable of rejecting CD48-deficient tumor cells (63, 66, 67). Other MHC-I independent interactions which educate NK cells include; SLAMF6/SLFMF6, NKRP1-B/Clr-b, TIGIT/CD155 (63). Regardless of the pathway utilized, educating NK cells is crucial to obtain functional mature and tolerant NK cells.

1.2.5 NK cell regulation by inflammatory cytokines and cross-talk with DCs and Neutrophils

Aside from being activated through activating receptors, NK cells can be activated by cytokines. These cytokines include; type I IFNs, IL-2, IL-12, IL-15 and IL-18 (68). Cross-talk between NK cells and immune cells such as Dendritic cells (DCs) or neutrophils is important for the release of the inflammatory/NK cell activating cytokines.

DCs are the predominant antigen presenting cell (APC) of the immune system. NK cells are capable of promoting DC maturation to promote Th1 priming through the release of IFN-γ

(69). In humans, activated NK cells were also capable of killing DCs which have not undergone normal DC-editing (DC maturation) via interactions with the NK activating receptor NKp30 (70, 71). However, through direct interactions and cytokine secretion DCs are also capable of promoting NK cell activation, proliferation, cytokine production and cytolytic activity (72). IL-12 can induce the secretion/production of IFN-γ from NK cells by binding the IL-12R. DCs have the ability to secrete IL-12 and IL-18 to directly promote IFN-γ production and to increase IL-12R expression on the surface of NK cells (70, 73). DCs also secrete the crucial NK cell cytokine IL-15 to promote NK cell proliferation, survival and activation (70). Plasmacytoid DCs (pDCs) play a crucial role in inducing NK cell cytotoxicity by producing high levels of IFNα/β (type 1 IFN) (70, 74). The IFN-β produced by the pDCs has also been reported to promote DC and NK cell secretion of IL-15 which is either trans-presented by DCs or cis-presented by NK cells to promote NK cell activation (70, 75, 76).

Neutrophils are the most abundant leucocytes in the body (77). They have a crucial role in combatting bacterial and fungal infections as well as for maintaining homeostasis and shaping host responses (78). A study by Jaegar et al. showed that neutrophil deletion impairs NK cell maturation, function and homeostasis (79). In addition, Riise et al. demonstrated that TLR-stimulated neutrophils instruct NK cells to respond to IL-12 and in so doing, promote DC maturation and adaptive T cell responses.(80). Neutrophils can also induce NK cell licensing and cytokine production (81, 82).

1.2.6 NK cell regulation by homeostatic IL-2/IL-15 cytokines

Several studies have been performed to identify the roles of IL-2 and IL-15 on NK cell development, maturation, activation and effector function. When the receptors IL-2Rβ or IL-2Rγc which are shared by the IL-2 and IL-15 were knocked out in mice, an important reduction of NK cells was observed in peripheral tissues (83-87). Similarly, IL-$15^{-/-}$ or IL-15R$\alpha^{-/-}$ had a significant reduction in NK cells but IL-$2^{-/-}$ and IL-2R$\alpha^{-/-}$ did not demonstrating that IL-15 is critical for NK development but IL-2 was not (83, 88, 89). Although not important in development, IL-2 promotes IFN-γ, cytotoxicity and NK cell proliferation demonstrating its important during inflammatory immune responses (83). IL-2 and IL-15 are both important for NK cell survival (90). IL-15 is also important for NK cell homeostasis, survival, activation, proliferation and cytotoxicity (83, 89, 91).

1.2.7 Signaling pathways downstream of IL-2/IL-15

The IL-2R and IL-15R share the same β- (CD122) and γ-chains which are constitutively expressed on the surface of NK cells (92, 93). However, upon cytokine binding, each recruits a specific α-chain (CD25 for IL-2, CD125 for IL-15) which promotes receptor specificity for the designated cytokine (93, 94). Upon receptor binding by either IL-2/IL-15, three downstream signalling cascades can be activated including the **(a)** JAK1-3/STAT5 pathway, **(b)** Ras-Ref-MEK-ERK (MAPK/ERK) pathway or the **(c)** PI3K-AKT-mTOR pathway (30). Signalling cascades and associated outcomes are depicted in Figure 2.

(a) Following IL-15/IL-15R or IL-2/IL-2R interaction, the receptor dimerizes inducing recruitment of JAK1 and JAK3 which auto-/trans-phosphorylate each other on their tyrosine residues (95). Once activated, the JAKs phosphorylate tyrosine residues on the receptor leading to the recruitment of STAT5 molecules via their SH2 domains (95, 96). The STATs are then tyrosine-phosphorylated by the JAKS leading to their activation (95, 96). Once activated the STAT5 molecules can dimerize and translocate to the nucleus to induce gene transcription (96). This pathway has an important role for NK cells as knock out of STAT5A resulted in a loss of NK cells in the periphery and a block in maturation in the NKP stage (97). STAT5 is also important for NK survival via its interaction with the anti-apoptotic factor MCL1 following IL-15 stimulation (98). Knock out of JAK1 reduced NK cell numbers, impaired NK cell development and resulted in complete ablation of NK cells in the peripheral lymphoid organs and impaired tumor surveillance (95). Patients with a mutation in STAT5B had a severe reduction in NK cells present (99). Altogether, these observations support the view that the JAK/STAT signalling pathway is crucial for the development and survival of NK cells.

(b) Following IL-15R/IL-2R receptor binding by IL-15 or IL-2, the receptor becomes phosphorylated and recruits Grb2 (93). Grb2 can bind to the guanine nucleotide exchange factor SOS which recruits and induces the Ras GTPase to exchange GDP for GTP (100). Once active, Ras can phosphorylate and thereby activate the serine/threonine kinase Raf (101). Active Raf kinase can then phosphorylate the serine/threonine/tyrosine kinase MEK to its active form which then phosphorylates the serine/threonine kinase Erk1/2 which can translocate to the nucleus and activates transcription factors to promote transcription (101). The Ras-Ref-MEK-ERK pathway is important for NK cell survival, as signalling downstream of IL-15 results in the activation of

Erk1/2, which phosphorylates the pro-apoptotic factor Bim targeting it for proteasomal degradation (102, 103). IL-2 activated human NK cells were shown to use the ERK pathway to secrete IFN-γ and to express CD25 and CD69 (104). In mice, it has been reported that the Ras-Ref-MEK-ERK induces cytotoxicity and cytokine release (105).

(c) Similar to the JAK/STAT and Ras-Ref-MEK-ERK pathway, binding of the cytokine to the receptor induces receptor phosphorylation which recruits and phosphorylates PI3K activating it. Once active, PI3K phosphorylates AKT which phosphorylates mammalian target of rapamycin (mTOR) (106). mTOR is sub-divided into two complexes; mTOR complex 1 (mTORC1) and mTOR complex 2 (mTORC2) (107). When phosphorylated, mTORC1 can phosphorylate/activate S6K and 4EBP1 and in so doing, controls translation (106). Specifically, S6K phosphorylates the ribosomal protein S6 (p-S6) which is part of the 40S subunit of the ribosome to promote ribosome biogenesis and protein synthesis (106). Phosphorylation of the translation initiation factor 4EBP1 allows it to bind eIF4e to increase RNA translation and ribosomal activity (106). mTORC1 also has roles in (i) upregulating nutrient transporters, (ii) lipid biosynthesis, (iii) autophagy and (iv) promoting expression of c-MYC and HIF-α (106, 108, 109). While less studied across all fields, mTORC2 has been highlighted for its roles in controlling cytoskeletal organization as well as for phosphorylating AKT to promote export of FOXO family transcription factors (106, 110). Using mTOR NK cell KO models, Marçais et al. have shown that following IL-15 stimulation, mTOR is required for NK cell maturation, proliferation, activation, reactivity as well as for effector function and killing (106). Moreover, they have shown that as NK cells mature, mTOR activity decreases but that as NK cells become activated mTOR activity increases (106). mTOR is also shown to become activated only at higher doses of IL-15 while the JAK1-3/STAT5 pathway is activated at lower doses of IL-15 (106). The immunosuppressive cytokine TGF-β which maintains homeostasis and prevents autoimmunity was shown to reduce NK cell development, metabolic activity, proliferation and NK cell cytotoxicity (111). Altogether, these studies demonstrate that mTOR integrates both pro/anti-inflammatory signalling in NK cells.

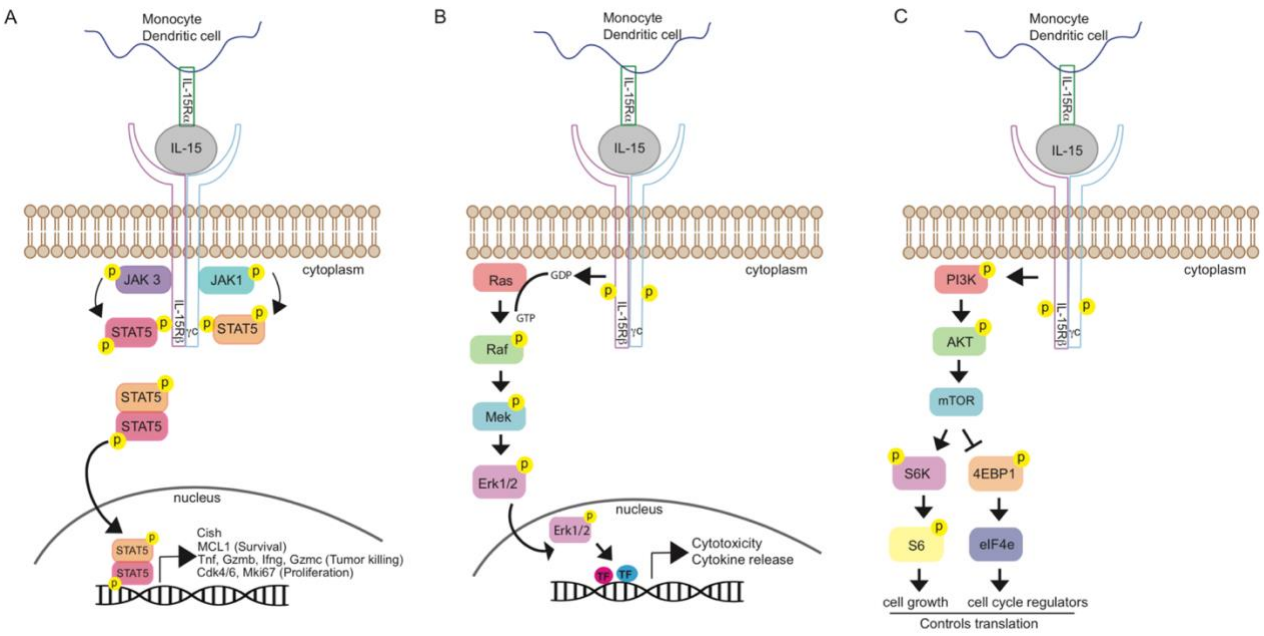

Figure 2 – IL-15 signaling pathways in NK cells
Under low doses of IL-15 such as in the context of homing, NK cells use the JAK/STAT and the Ras-Ref-MEK-ERK pathway. During development or in the context of infection, increased levels of IL-15 will be present and will also induce the activation of the mTOR pathway. Arrow from the receptor illustrates that there are steps in between receptor binding and downstream signalling. Figure was developed using the following publication (83, 106, 112-115).

1.3 NK cell responses

1.3.1 Cytotoxicity

NK cells are known for both their cytotoxic and regulatory properties. When activated, NK cells can exert these functions to target aberrant cells; virally infected or tumorigenic cells. They release cytolytic molecules such as granzyme B and perforin to directly kill infected cells (116). NK cells are one of the major producers of granzyme B and perforin (117). Following target cell recognition, a lytic synapse is formed between the NK cell allowing for directed secretion towards the target cell without impact neighboring cells (117). Formation of synapse is associated with changes in the NK cell structure and organization of organelles. Microtubules, the Golgi and cytolytic granules are translocated to the synapse (116, 118, 119). At the synapse, cytoplasmic granules containing perforin and granzyme B are released (116). Perforin is a glycoprotein which induces pore formation in the cell membrane of target cells thereby allowing for passive, non-selective entry of enzymes, ions, water and small-molecules which results in destruction of cell

integrity (116, 120). The serine protease, Granzyme B is a primary mediator of target cell death (121). Following perforin pore formation, Granzyme B enters the targets cell cytoplasm, initiates caspase cleavage which in turn causes apoptosis (121, 122).

1.3.2 Cytokine secretion

NK cells have the ability to interact with other immune cells to induce inflammation and immune responses by cell-cell contacts or the release of soluble factors. Activated NK cells are major producers of IFN-γ and TNF-α; pro-inflammatory cytokines which are secreted into the environment to promote activation/maturation of dendritic cells, neutrophils, macrophages and T cells (72, 123). Early production of IFN-γ by NK cells is necessary for proper Th1 polarization (124). Moreover, studies showed that *in vitro*, NK cells were able to promote DC maturation due to cell-cell contact and the production of IFN-γ and TNF-α which ultimately allows for indirect Th1 polarization (69). NK cells have also been reported to produce GM-CSF, IL-5, IL-13, IL-19, IL-22 which modulate immune responses (72, 123). *In vitro*, activated NK cells regulated neutrophil survival and activation by secreting GM-CSF and IFN-γ (72, 125). In murine models, NK cells producing IL-22 stimulated the recruitment of neutrophils to the site of infection with MCMV (70, 72). Human/mouse NK cells are also known for producing chemokines. Specifically, human NK cells have been shown to produce chemokines such as XCL1, CCL1, CCL3, CCL4, CCL5, CCL22, CXCL8 when activated to recruit other effector cells to the site of infection/inflammation (126).

1.3.3 NK cell memory

In the past, it was believed that only adaptive immune cells (T and B cells) could generate memory cells which were antigen specific and produced amplified responses upon re-exposure. However, innate immune cells such as NK cells were thought to respond quickly and consistently despite having been previously exposed to the antigen. However, in recent years, it was identified that NK cells with a memory-like phenotype can develop **(a)** in response to viral infection, **(b)** in response to haptens and **(c)** cytokine-induced cell memory.

(a) NK cell memory in response to viral infection: In response to viral infection, NK cells can develop into memory NK cells. One of the best studied models is using MCMV. Memory NK cells can develop in response to MCMV due to the interaction of m157 viral protein with Ly49H (127-129). This was confirmed by the observation that MCMV lacking m157 did not

produce memory NK cells (127, 129). Following adoptive transfer of $Ly49H^+$ NK cells into $Ly49H^{-/-}$ mice, the mice were infected MCMV; they observed an expansion of $Ly49H^+$ NK cells to control the infection (127). Once the infection was cleared, the cells underwent a contraction phase. A portion of NK cells survived the contraction and established a pool of long-lived memory cells which could undergo secondary expansion, had enhanced effector function, provided increased protection against virus challenge and had a distinct transcriptional signature from naïve NK cells (127). It is believed that like for T cells three signals are required for the generation of memory NK cells. The three signals consist of (i) antigen-receptor engagement, (ii) co-stimulatory signalling and (iii) pro-inflammatory cytokine signalling (127). During MCMV infection the signals which would induce NK cell memory include; (i) Ly49H-m157 interaction, (ii) DNAM-1 and (iii) IL-12, IL-33, IL-18, STAT4, MyD88 and Zbtb32 (127). During the contraction phase, NK cells down regulate the anti-apoptotic molecule BCL-2 and use Bim-mediated signalling to control the quantity of memory NK cells (127). NK cell memory formation has also been elucidated for herpes simplex virus 2 (HSV-2) and vaccinia virus as with both infections, re-challenge promoted enhanced IFN-γ production and viral protection (127). Transfer of NK cells previously exposed to influenza infection injected into naïve mice display a memory like phenotype and clear the new infection (127). Therefore, NK cell memory formation can occur in response to viral infection.

(b) NK cell memory in response to haptens: A hapten is a small molecule that when coupled with a carrier protein (hapten specific antibodies) is referred to as a conjugate (130). When conjugated, the hapten and the carrier protein become immunogenic and can elicit a directed immune response (130). Haptens were the first molecules identified to induce a form of memory NK cells (127). A contact hypersensitivity (CHS) response is an adaptive immune-mediated delayed type of hypersensitivity reaction. In the absence of T and B cells (Rag2-deficient mice or SCID mice), hepatic but not spleen NK cells could mediate a hapten specific CHS response which disappeared in Rag2-deficient, γc-deficient mice lacking T, B and NK cells (45, 127, 131). More interesting is the fact that $CD45^+$ liver NK cells expressing CXCR6 and Thy-1 mediated the response (45). When the receptor CXCR6 or its ligand were altered, the hapten recall response did not occur as the NK cells could not persist (45). Moreover, the hapten monobenzone can induce hepatic NK cell memory but it requires NLRP3 inflammasome in tissue-resident macrophages

(132). Some studies have shown that liver NK cells expressing Ly49C-I were important to mediate long-lived, antigen-specific recall responses (131).

(c) Cytokine induced NK cell memory: Cytokines alone are capable of inducing NK cell memory-like phenotypes. In both mice and humans, NK cells cultured with IL-15, IL-12 and IL-18 responded better to cytokine or activating receptor stimulation when adoptively transferred into Rag-deficient mice (17, 127, 133). Moreover, they displayed increased IFN-γ production but did not express increased cytotoxic potential (17, 127, 133). The memory NK cells produced in a cytokine induced setting have been shown to be different than those produced from a viral response. Studies have shown that pre-stimulating the NK cells with the cytokine cocktail depicted above can play an important in anti-tumor responses (127). During viral infections, cytokine-induced NK cell memory-like cells can be produced. Cytokines will activate NK cells in the bone marrow prior to going to the site of injury/inflammation (134). Although the cells were activated in the context of an influenza infection, the NK cells were able to more effectively respond to respiratory syncytial than naïve cells (127, 134).

1.4 The mouse model of cytomegalovirus infection to understand NK cell biology

1.4.1 Cytomegalovirus

Cytomegalovirus (CMV) is a double stranded DNA virus in the Herpesviridae family (19, 135). The viral structure consists of a core with the genome, an icosahedral capsid, an amorphous protein coat (tegument), and an envelope (19). The capsid is made of capsomers and the envelope is made of a glycoprotein lipid bilayer (19).

The Herpesviridae is divided into 3 groups (α, β, γ Herpesviruses) of which CMV is a member of the β-group (19). In people, human cytomegalovirus (HCMV) causes primary infection and then remains as a life-long latent infection in immunocompetent hosts (19, 135). Immunocompromised hosts can have severe infections with CMV (19). HCMV typically causes infection in the salivary glands (19, 135).

Mice can be infected by the mouse cytomegalovirus (MCMV). In 1954, Margaret Smith isolated MCMV from the salivary glands of infected laboratory mice which is now termed the Smith strain (136). MCMV mouse infection is a well-established model to study the role of NK cells in virus control (137). Acute infection with MCMV is controlled by NK cells and $CD8^+$ T

cells, however, the importance of each cell type depends on the mouse model (138). B6 mice have the Ly49H receptor allowing the NK cells to bind the m157 viral protein thereby controlling the viral infection however, BALB/c and 129/J mice lack the Ly49H receptor on NK cells therefore, antiviral responses are predominantly provided by $CD8^+$ T cells (39, 138). BALB/c and 129/J mice are susceptible to MCMV infection (39, 138). In B6 mice, MCMV infection will result in non-selective and selective NK cell activation (54, 139, 140). During the non-selective activation phase, pro-inflammatory cytokines, IL-12 and IL-15 will be produced to stimulate both $Ly49H^-$ and $Ly49H^+$ NK cells to proliferate and produce IFN-γ (54, 139, 140). However, selective activation of $Ly49H^+$ NK cells occurs when Ly49H binds m157 to drive $Ly49H^+$ NK cells to proliferate and release cytolytic molecules that control MCMV infection (54, 139).

1.4.2 Gnl1^{365X} mutation results in an NK cell deficiency

Our laboratory has used random chemical mutagenesis in mice and challenge with MCMV to identify novel regulators of NK cells. Following an *N*-ethyl-*N*-nitrosourea (ENU) induced mutagenesis screen, we identified a pedigree with severe susceptibility to MCMV infection due to a loss of function mutation in the gene, *Guanine nucleotide binding protein like 1* (*Gnl1*) (18). A T-A mutation in the 8th exon of *Gnl1* changes the amino acid cysteine to a premature stop codon at position 365 (mutant = *Gnl1*$^{C365X/C365X}$, short-hand = *Gnl1*^{C365X}), truncating the functional GNL1 polypeptide (18). GNL1 consists of 607 amino acids and is expressed both in the nucleus and cytoplasm of cells (141). The sequence of *Gnl1* is highly conserved across evolution making mouse models a relevant way to study *Gnl1* as a proxy for humans. The *Gnl1*^{C365X} mice are leukopenic however the mutation results in an NK cell specific deficiency as $CD4^+$ T cells, $CD8^+$ T cells, B cells, ILCs and myeloid cell (monocytes and macrophages) proportions remain unchanged (18). The mutation is recessive as heterozygous mice display wild type proportions of NK cells. Furthermore, when challenged with Herpes simplex virus 1 (HSV-1), *Gnl1*^{C365X} mice were not susceptible further displaying that the mice do not have a generalized immunodeficiency (18). We identified that their inability to provide sufficient protection against MCMV was not a result of their inability to produce cytokines (IFN-γ) or proliferate in response to infection but a result of not having enough NK cells to control the infection (18). Next, we identified that *Gnl1*^{C365X} mice had a higher proportion of immature NK cells and underwent increased apoptotic cell death via caspase 3 (18). The mutant NK cells were incapable of efficiently responding to

stimulation from their lineage determining, homeostatic and activating cytokine IL-15. In addition, following IL-15 stimulation for 2, 4 and 6 days, *Gnl1*^{C365X} NK cell numbers were reduced and associated with decreased survival and Ki67 expression further highlighting their inability to effectively respond to IL-15, increased cell death and reduced proliferative capacity.

1.5 The GNL1 gene family

GNL1 is a part of the YawG/YlqF/HSR1-MMRI large GTPase family (142). This family of GTPases is conserved across evolution from prokaryotes to mammals (141, 142). The members include GNL1, GNL2, GNL3 and GNL3L (141, 143). They are circularly permutated GTPases with the guanine nucleotide motifs arranged as G5-G4-G1-G2-G3 instead of the typical G1-G2-G3-G4-G5 arrangement found in classical GTPases (141, 144). Recently, Krishnan et al. demonstrated that the interaction of human *Gnl1* with small ribosomal unit 20 (RPS20) was important to promote cell proliferation and survival (141).

Although mouse *Gnl1* is not well defined, other species encode homologs; GNL1 related proteins have been highlighted for their role in ribosome biogenesis, controlling cell cycle, stem cell biology and embryonic development (142, 143). The ribosome is a complex structure composed of numerous proteins and nucleic acids which are involved in mediating translation of messenger RNA into proteins (145). Ribosome biogenesis is the tightly regulated process that requires the cooperation of a multitude of factors for the synthesis and assembly of the ribosome and its two main components, the large and small ribosomal subunits (145). Defects in ribosome biogenesis trigger a p53-activating checkpoint signaling pathway, often referred to as the ribosomal stress checkpoint pathway (146, 147). Activation of the tumor suppressor p53 induces transcription as well as a number of downstream effects including cell cycle arrest and/or apoptosis (148).

In *Bacillus subtilis,* the ribosome biogenesis GTPase A (RbgA) is required for the later steps of the large ribosomal subunit assembly in bacteria (149). In yeast, it was observed that large 60S subunit nuclear export GTPase 1 (LSG1) is required for nuclear export and further maturation in the cytoplasm of the large ribosomal subunit (150). In the retina of zebrafish, the absence of GNL2 or GNL3 inhibits cells from exiting the cell cycle as a result of aberrant expression of cell cycle regulators (151, 152). GNL3 (nucleostemin) or GNL3L disruption causes an increase in p53-dependent cell cycle blockage (G2/M arrest) via the inhibition of MDM2 in a L5/L11 dependent

manner (151). These findings support the study by Morgado-Palacin et al. which demonstrated that ribosomal stress can specifically induce p53-dependent apoptosis (147).

Chapter 2 – Rationale and Objectives

2.1 Rationale and Hypothesis

In our laboratory, we observed that *Gnl1*^{C365X} NK cells had increased active caspase 3 expression. Although the mechanism of GNL1 in NK cell survival is not completely understood, there exists a link between ribosomal stress, p53 and cell cycle/cell death that may underlie the NK cell deficiency in *Gnl1*^{C365X} mice. Therefore, we hypothesize that the *Gnl1*^{C365X} mutation perturbs p53 activation as well as cell cycle and ribosomal protein gene expression in NK cells.

2.2 Objective and aims

The overall objective is to understand the mechanism by which mutation of GNL1 leads to the NK cell deficiency observed. To test our hypothesis, we have designed two experimental aims;

Aim 1: To identify differentially expressed ribosomal protein genes which result in *Gnl1*^{C365X} NK cell deficiency. This aim will first require the development of a method to sort *Gnl1*$^{+/+}$ and *Gnl1*^{C365X} NK cells. We will perform several quality control steps to confirm the RNA obtained is of good quality. Next, we will perform RNA sequencing to obtain a dataset which will then be analyzed using an RNA-sequencing pipeline to identify differentially expressed genes. Gene ontology and Gene set enrichment analysis (GSEA) will be performed to identify terms and signatures respectively. Moreover, we will highlight the genes underlying the enriched signatures to identify gene candidates associated with the NK cell deficiency.

Aim 2: To characterize the impact of p53 ablation in the impaired NK cell response observed in *Gnl1*^{C365X} mice. For this, we will generate *Gnl1*^{C365X}*Trp53*$^{-/-}$ mice and compare how they respond to MCMV infection relative to *Gnl1*$^{+/+}$, *Gnl1*^{C365X}, and *Gnl1*$^{+/+}$*Trp53*$^{-/-}$ mice. We will also validate preliminary experiments performed in the laboratory demonstrating the rescue of the NK cell deficiency and caspase 3 levels. We will further validate whether *Trp53*$^{-/-}$ can overcome the maturation and receptor defects identified in *Gnl1*^{C365X} mice.

Chapter 3 – Materials & Methods

3.1 Experimental animal and ethics statement

C57BL/6J and C57BL/10J mice were purchased from Jackson laboratories (Bar Harbor, Maine, USA). *Gnl1*^{C365X} mice were identified in an ENU chemical mutagenesis screen on a mixed B6/B10 background, and back-crossed at least 4 times to a B6 background (93.5% homozygous B6). Littermate wild-type (*Gnl1*$^{+/+}$) and homozygous mutant *Gnl1*^{C365X} mice, ranging from 7 to 14 weeks of age, and including both male and females, were used in all subsequent experiments. p53 heterozygous mice, which had been maintained in a B6 background, were kindly provided by Dr. N. Sonnenberg. Breeding was done to generate *Gnl1*$^{+/+}$*Trp*53$^{-/-}$ or *Gnl1*^{C365X}*Trp*53$^{-/-}$ mice. All animals were housed and maintained at McGill University. All animal procedures were carried out in accordance with the Canadian Council on Animal Care and were approved under protocol number 4792 by the McGill University Animal Care Committee.

3.2 Viral stock and mouse infection

A mouse cytomegalovirus (MCMV) smith strain was purchased from the American Type Culture Collection (ATCC VR-1399, lot 1698918). The strain was propagated as described (153).

A survival study using mice 8 to 12 weeks in age were infected with 4,000 PFU i.v. of MCMV and monitored daily up to day 14 post-infection. Mice were euthanized at clinical end point (15% weight loss or body correction score less than 2 or piloerection or ungroomed appearance or hunched posture or anti-social behaviour or lethargy).

3.3 Genotyping

Ear punches obtained from mice were digested in DNA digestion buffer with Proteinase K for a minimum of 2 hours at 55°C. The samples were placed at 98°C for 10 minutes to deactivate the Proteinase K.

3.3.1 Gnl1 genotyping - To determine the genotype of *Gnl1*$^{+/+}$, *Gnl1*$^{+/C365X}$ and *Gnl1*^{C365X} mice, PCRs are run using the forward primer 5'-GGGTGGTGACTATTGGCTGT-3' (GNL1_F1) for wild-type or 5'- GGGTGGTGACTATTGGCTGA-3' (GNL1_F2) for mutant mice with the reverse primer 5'- GCCACAGCTCACCTCCATCT-3' (GNL1_R) ordered from BioCorp. The master mix consists of 10X buffer, dNTPs, forward and reverse primers, 50% glycerol, miliQ H_2O and Taq polymerase. 2μL of the digested sample is used for genotyping. PCR reactions are then

run on a 1% agarose gel containing ethidium bromide in TAE buffer in gel chambers. Bands were visualized on the Molecular Imager® Gel Doc™ XR system (Bio-rad). PCR run: 95°C for 2 min, 30 cycles of 95°C for 30 sec, 66°C for 20 sec, 72°C for 30 sec followed by a cycle at 72°C for 3 min. A band 320 bp in size observed in the wild-type gel signifies that the mouse has a wild-type allele. A band 320 bp in size observed in mutant gel signifies that the mouse has a mutant allele. If the sample has bands in both the wild type and the mutant PCRs, the mouse is heterozygous for *Gnl1*, if the mouse has a wild type band but no mutant band it is homozygous wild type for *Gnl1* and if the mouse has a mutant band but not a wild type band it a *Gnl1* homozygous mutant.

3.3.2 P53 genotyping – To determine if mice are $p53^{+/+}$, $p53^{-/+}$ or $p53^{-/-}$, a PCR was run using three primers; 5'- ACA CAC CTG TAG CTC CAG CAC-3' (P5314F), 5'- AGC GTC TCA CGA CCT CCG TC-3' (P53E5R) and 5'- GTG TTC CGG CTG TCA GCG CA-3' (OPT-21) ordered from BioCorp. The master mix consists of; 10X buffer, dNTPs, the primers mentioned above, miliQ H_2O and Taq polymerase. 2μL of the digested sample is used for genotyping. PCR is run on a gel and visualized as for *Gnl1*. PCR run; 95°C for 3 min, 30 cycles of 95°C for 20 sec, 66°C for 20 sec, 72°C for 1 min followed by a cycle at 72°C for 5min. $p53^{+/+}$ mice have a 520 bp band, $p53^{-/-}$ have a band 730 bp in size while $p53^{-/+}$ mice have both the 520 bp and 730 bp band.

3.4 Splenocyte preparation

To obtain single cell spleen suspensions, spleens from $Gnl1^{+/+}$ and $Gnl1^{C365X}$ mice were harvested in complete RPMI (cRPMI); RPMI media (Wisent Inc., 350-000-CL) supplemented with 10% heat-inactivated (HI) FBS (GE health line, SH30396.03), 1x HyClone Non-Essential Amino Acids (ThermoFisher, SH30238.0), 50 μM 2-mercaptoethanol (ThermoFisher, 21985-023), 1mM HyClone™ sodium pyruvate (GE Health Line, SH30239) and 1% Penicillin and Streptomycin (Wisent Inc., 450-201-EL). Spleens were macerated through 70 μm cell strainers and they were treated with Red Blood Cell Lysis Buffer Hybri-Max™ (Sigma, R7757). The cell suspensions were then filtered through a 70 μm cell strainer to obtain single cell suspensions.

3.5 *Ex-vivo* treatment with actinomycin D

$4x10^6$ spleen cells were plated per well in a 24 well plate in a final volume of 2mL (cRPMI +/- treatments). The cells were subjected to one of six treatments; (1) no treatment, (2) 10ng/mL of actinomycin D (ThermoFisher, 11805017), (3) 200ng/mL of actinomycin D, (4) 2ng/mL of IL-

15 (PeproTech, 210-15), (5) 2ng/mL of IL-15 with 10ng/mL of actinomycin D and (6) 2ng/mL of IL- 15 with 200ng/mL of actinomycin D. Cells were maintained for 24 hours or 48 hours at 37°C with 5% CO_2. Cells were then stained and processed on the BD FACSCanto II (BD Biosciences) as described in the splenocyte preparation, flow cytometry and cell sorting section.

3.6 Flow cytometry and cell sorting

For flow cytometric analysis, single cell spleen suspensions were resuspended at 25 x 10^6 cells/mL in cRPMI. 5 x 10^6 cells were seeded per well of a 96 well round bottom plate and washed using FACS buffer (PBS containing 2% HI FBS and 2mM EDTA). Extracellular staining was performed in FACS buffer for 20 minutes at 4°C followed by viability staining using fixable viability dye eFluor 506 (eBioscience) for 15 minutes at 4°C. Fixed samples were prepared by incubating cells at 4°C for 20 minutes with 2% paraformaldehyde (PFA) (16% PFA stock solution, Cedarlane, 15710EM). For detection of apoptosis, fixed cells were additionally stained with CaspGLOW fluorescein active Caspase-3 Staining Kit (eBioscience, 88-7004-42) following manufacturer's protocol. Moreover, non-fixed cells were stained with AnnexinV/PI kit (BD Bioscience) following the manufacturer's instructions. Samples and compensation controls were run on the BD FACSCanto II (BD Biosciences) and analyzed using FlowJo software. Antibodies used for staining are outlined in Table A1.

For cell sorting, single cell spleen suspensions were stained at a concentration of 5x10^6 cells/50 µL using antibodies specific to NK1.1, NKp46, DX5, CD3, CD19 (Table A2). 5 minutes prior to sorting, the cells were stained with DAPI (Sigma, D9542) at a concentration of 1µg/mL to differentiate viable cells from dead cells. Cells were sorted on the BD FACSAria™ III (BD Biosciences) using a 70 µM nozzle with a pressure of 70 psi. Compensations were performed directly on the machines during the sort. Sorting gating strategy used to sort singlet viable NK cells selected were $DAPI^-$ $NK1.1^+$ $NKp46^+$ $DX5^+$ $CD3^-$ $CD19^-$ similar to Quatrini et al. (154). Gating strategy; Lymphocytes (FSC-A by SSC-A), Singlets (FSC-A by FSC-H), Live cells (FSC-A by $DAPI^-$), NK cells ($NK1.1^+$ by $CD3^-CD19^-$ → $NK1.1^+$ by $NKp46^+$ → $CD3^-CD19^-$ by $DX5^+$) (Fig. A2).

3.7 RNA preparation and extraction

Cells were sorted to purity as described in the flow cytometry and cell sorting section and collected in PBS containing 20% HI FBS and 1x NEAA. Cells were pelleted and washed with PBS. Cells were then re-pelleted and resuspended in lysis binding solution as per the manufacturer's protocol, vortexed for 30 seconds and left to sit for 4 min 30 seconds at room temperature prior to quick freeze on dry ice and storage at -80°C (ThermoFisher, AM1830). RNA was then extracted as per manufacturer's protocol using the kit along with the DynaMag™-2 (Life Technologies, 12321D) and the Eppendorf™ Mixmate™ (Thermo Fischer, 2137900) set a speed of 1650 rpm for the entire experiment. RNA was collected in 20 μL of elution buffer; 1.2 μL was set aside for quality control; the rest was kept for sequencing.

3.8 Quality control, cDNA library preparation and sequencing

The aliquot of RNA stored for quality control was sent to the Molecular Biology platform located at the Montreal Clinical Research Institute (IRCM). Samples were run on a Bioanalyzer (Agilent Technologies) to obtain an RNA integrity score (RIN) which allows for the determination of the quality of RNA and the presence of contamination (e.g. genomic DNA). To be considered for RNA-sequencing, samples needed to have a minimum RIN score of 7.5. The RIN scores for the selected samples (*Gnl1*$^{+/+}$ 1-3 and *Gnl1*^{C365X} 1-3) can be found in Table A3. Selected samples were rRNA depleted prior to the production of the cDNA library. The KAPA stranded RNA-seq kit was used to produce the cDNA library. Approximately 20 ng of RNA was used to produce the libraries. 11 cycles of PCR enrichment were performed. Illumina HiSeq 4000 paired-end 50 (PE50) sequencing was used to produce the data set. RNA-sequencing results and experimental set up are further depicted in Table A4.

3.9 RNA-sequencing pipeline

FASTQ files obtained following sequencing were provided to the Canadian Centre for Computational Genomics (C3G) and run on the workflow management system GenPipes. Specifically, the RNA-sequencing pipeline was used. Adaptor sequences and low-quality reads were trimmed using Trimmomatic; samples required a minimum phred score of 30 and a minimum read length of 32 in order to be kept for further downstream analysis. Moreover, any sample containing adaptor sequences were removed. The trimmed readset for each sample was aligned to the Mus_musculus genome assembly GRCm38 using the splice-aware aligner STAR. A threshold

of greater than or equal to 9 CPM to the sum of 3 samples for one group (wild type or mutant) was set. Next, EdgeR and DeSeq2 Bioconductor packages were used to assess differential gene expression statistically.

3.10 Analysis of dataset

Genes were identified as differently expressed (DEG) in the dataset if they had a Log2FC cut-off of > |1.5| and an adjusted p-value <0.05 in both EdgeR and Deseq2 Bioconductor packages. Gene ontology (GO) was performed using the bioinformatics tool DAVID (FDR ≤ 0.05) (155, 156). GSEA analysis was performed on the GSEA desktop version 3.0. software from the BROAD institute (157, 158). Requires Java8 to run. A dataset file (.txt), phenotype labels file (.cls) and an annotation file (.chip) were generated and loaded into the application. All 10871 expressed genes having met a sum of 9 CPM or higher in either *Gnl1*^{C365X} or *Gnl1*$^{+/+}$ sample groups were queried for enriched gene sets, against two available GSEA gene set collections (C7.all.v6.2.symbols.gmt immunological signatures, C2.cp.kegg.v6.symbols.gmt KEGG pathways), and with 1000 permutations on gene sets. The immunological signatures collection contains 4872 gene sets and the KEGG pathway collection contains 186 gene sets. Gene sets that met an adjusted p-value cut-off of < 0.01 were identified as being significantly enriched, and the top 25 highest-ranking leading-edge genes that drove enriched signatures were identified. Gene expression for DEG and leading-edge genes were visualized with heatmaps created with the "gplots" package in R, as further described in each the figure legend. Gene tracks showing the abundance of mapped paired-end reads were visualized using IGV (159-161).

3.11 Statistics

Data were analyzed using the GraphPad Prism Software version 6.0 or statistical packages specified for DEG or GSEA analysis. P-values lower than 0.05 were considered as statistically significant, or as indicated in each figure legend. (*p<0.05, **p <0.01, ***p<0.001, ****p <0.0001).

4.1 *Gnl1*^{C365X} NK cells undergo increased apoptotic cell death

Our laboratory has previously reported that *Gnl1*^{C365X} mice are susceptible to MCMV as a result of a reduction in the proportion and number of NK cells and not due to their ability to initiate a cytotoxic/regulatory response (18). Moreover, the NK cell specific deficiency is associated with increased active caspase 3 expression; a caspase involved in the execution of apoptotic cell death downstream of intrinsic triggers such as activation of p53. Our first goal was to validate the NK cell deficiency and the cell death phenotype observed in the *Gnl1*^{C365X} mice. For this, we used flow cytometric analysis to study NK cells, gating for singlet, lymphocyte and viable cells, which were subsequently gated using the three canonical C57BL/6 NK cell markers: CD49b, NK1.1 and NKp46 (Fig. A1-A). We confirmed that there was a significant decrease in the proportion of CD49b^{+}CD3^{-} , NK1.1^{+}CD3^{-} and NKp46^{+}CD3^{-} *Gnl1*^{C365X} splenic NK cells as compared to *Gnl1*$^{+/+}$ NK cells (Fig. 3A and B). NK cell numbers were also significantly decreased in mutant mice compared to wild-type littermates (not shown). Moreover, we confirmed that there was increased active caspase 3 expression in the *Gnl1*^{C365X} NK cells (Fig. 3C). Of note, no difference in cell percentage or caspase 3 expression was observed in B, CD4^{+} or CD8^{+} T cells as previously reported further demonstrating the deficiency is NK cell specific (data not shown). To further confirm the apoptotic phenotype, observed via caspase 3 we performed annexin V (AnnV) – Propidium Iodide (PI) staining. We observed no difference in the percentage of total viable cells (AnnV^{-}PI^{-}) nor in the percentage of dead cells (AnnV^{+}PI^{+}) however, we did observe an increase in apoptotic cell death (AnnV^{+}PI^{-}) in the *Gnl1*^{C365X} NK cells as compared to the wild-type (Fig 3D). Thus, at steady state, *Gnl1*^{C365X} mice have an NK cell deficiency associated with increased apoptotic cell death.

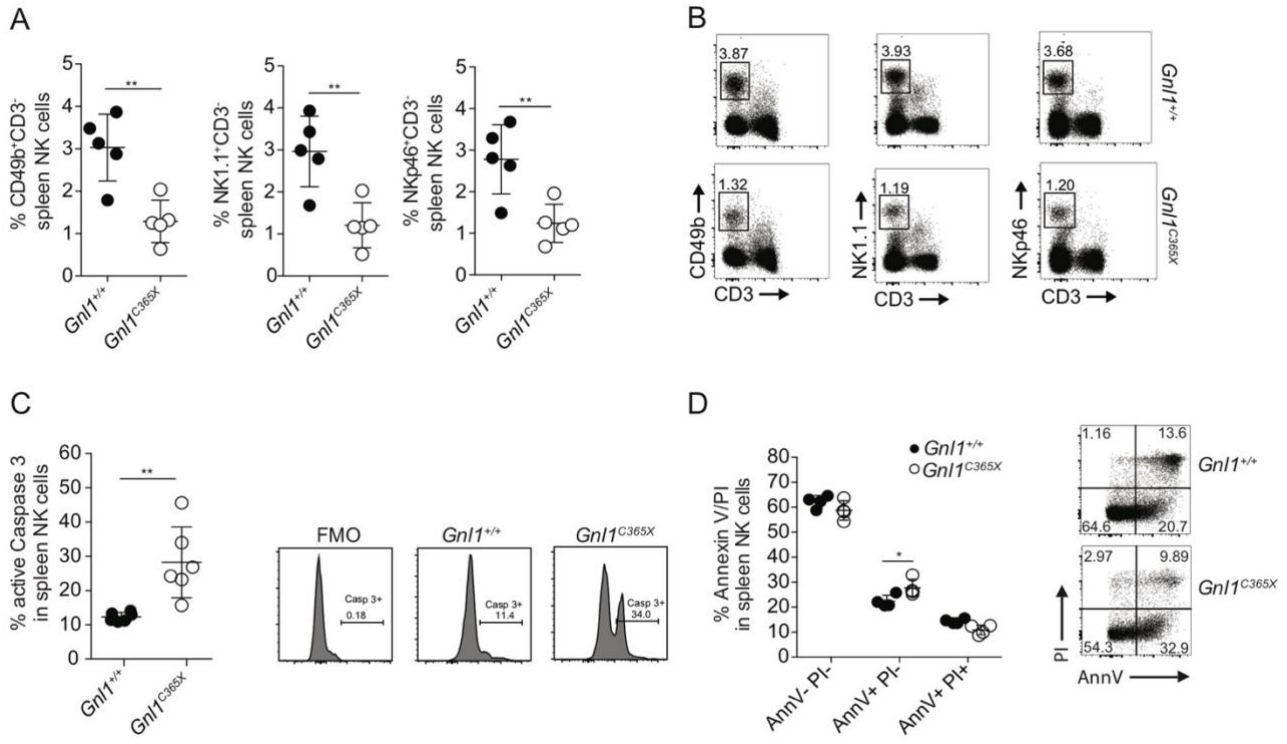

Figure 3: *Gnl1*^{C365X} NK cells undergo increased apoptotic cell death

Flow cytometric analysis was performed on *Gnl1*$^{+/+}$ and *Gnl1*^{C365X} splenocytes. **(A)** Graphic representations of the proportion of CD49b^{+}CD3^{-}, NK1.1^{+}CD3^{-}, NKp46^{+}CD3^{-} splenic NK cells. (n = 5 mice/genotype). **(B)** representative flow plots for *Gnl1*$^{+/+}$ and *Gnl1*^{C365X} NK cells stained with the NK cell markers described in (A). **(C)** Graphic and representative flow plots for the expression of active caspase 3 on NK1.1^{+}CD3^{-} spleen cells. Fluorescence minus one (FMO) plot is also shown. Two-tailed unpaired Student's t-test (n = 6 mice/genotype). **(D)** Graphic and representative plots of *Gnl1*$^{+/+}$ and *Gnl1*^{C365X} splenic NK cells (NK1.1^{+}CD3^{-}) stained for annexin V and PI. AnnV^{-}PI^{-} (live cells), AnnV^{+}PI^{-} (apoptotic cells) and AnnV^{+}PI^{+} (dead cells). Two-way ANOVA with Sidak's multiple comparisons. (n = 4 mice/genotype). **(A-D)** All data shown as mean ± SD. P-values; *p<0.05, **p<0.01.

4.2 GNL1-dependent pathways in NK cells

To obtain a better understanding of the molecular mechanisms underlying the NK cell deficiency seen in *Gn1l*^{C365X} NK cells, we performed RNA-sequencing to identify differentially expressed genes (DEGs). The first step was to obtain a pure population of NK cells. Similar to Quatrini et al. (154), we used flow cytometric staining to sort conventional NK cells from the spleen of C57BL/6 mice expressing NK1.1, NKp46 and DX5 (Fig. A2, Table A2). Using these three murine NK cell markers together excludes ILCs from the population being sorted since ILCs do not express DX5 and NKp46/NK1.1 expression is dependent on the ILC type (27, 162). We also gated for CD3$^-$CD19$^-$ cells to exclude T and B cells from being included in the analysis. Finally, we used the DNA stain DAPI to select live cells, in order to yield good quality RNA for downstream analysis (Fig. A2). Using the staining depicted above, we were able to obtain between 85-91% NK cell purity for the samples with the exception of *Gnl1*^{C365X} sample 1 which had a purity of 77.9% (Table A3). Purified cells were subsequently used to prepare RNA for the synthesis of a cDNA library; each cDNA fragment was used for the sequencing of 50 bp from each end (50 bp-paired end) using the HiSeq 4000 technology. We obtained a total of 323,178,640 PE total reads, which represents between 47-62 million paired end reads per sample (Table A4, A5). The samples were analyzed by the C3G core using an established pipeline for sequence quality control, genome mapping and transcript counting and identification of DEGs. Briefly, the reads had very good sequence quality as indicated by a Phred quality scores of 38. The raw reads needed to be trimmed to remove low quality reads/bases and adaptor sequences. Between 90.7-97.7 % of the reads survived trimming. Using the splice aware aligner STAR, the surviving reads were mapped to the mouse genome. Between 55-73.7 % of reads aligned of which 68.9-78.6 % aligned to exons (Table A5). All steps performed yielded results in ranges accepted within the field (163).

4.3 Gene ontology on 143 DEGs highlights differences in cell cycle processes

In order to identify differentially expressed genes which could be altered as a result of the *Gnl1*^{C365X} NK cells, the C3G pipeline uses the EdgeR and Deseq2 bioconductor packages. First, we had to define a minimum count per million (CPM) reads that would define an expressed gene to determine the total number of genes expressed. Using a filter of a sum CPM of 9 in either the wild-type or the mutant group, a total of 10,857 genes were identified in NK cells. Next, we defined a DEG as a gene showing a fold change of greater than the absolute value of 1.5 and a p-value of

<0.05. When this filter was applied, 209 DEGs were identified using EdgeR and 156 DEGs were identified using Deseq2, of which 143 DEGs were identified by both programs (Fig. 4A). Of the 143 DEGs, 84 genes (red) were upregulated 59 genes (blue) were identified as downregulated in *Gnl1*^{C365X} NK cells as compared to *Gnl1*$^{+/+}$ control while all the remaining 10,714 genes (black) were not considered as differentially expressed based on the selected cut-offs (Fig. 4B). This is further illustrated using a heat map demonstrating expression of genes in *Gnl1*^{C365X} as compared to wild-type (Fig. 2C). To determine whether the 143 DEGs belong to shared pathways, we used DAVID to obtain Gene Ontology (GO) annotations. Using an FDR <0.05, 50 GO terms were identified of which 10 were selected to represent annotations associated with the DEGs. The terms were associated with cell cycle processes and cell division which highlighted a role for cell cycle (Fig. 4D). In addition, it is important to note that *Gnl1* was the gene with the most statistically significant difference between wild-type and mutant NK cells (Fig. 4B). There was a 1.5-fold reduction in gene expression in *Gnl1*^{C365X} NK cells as compared to wild-type which further validates that *Gnl1* expression is altered in the mutant NK cells (Fig. 4E).

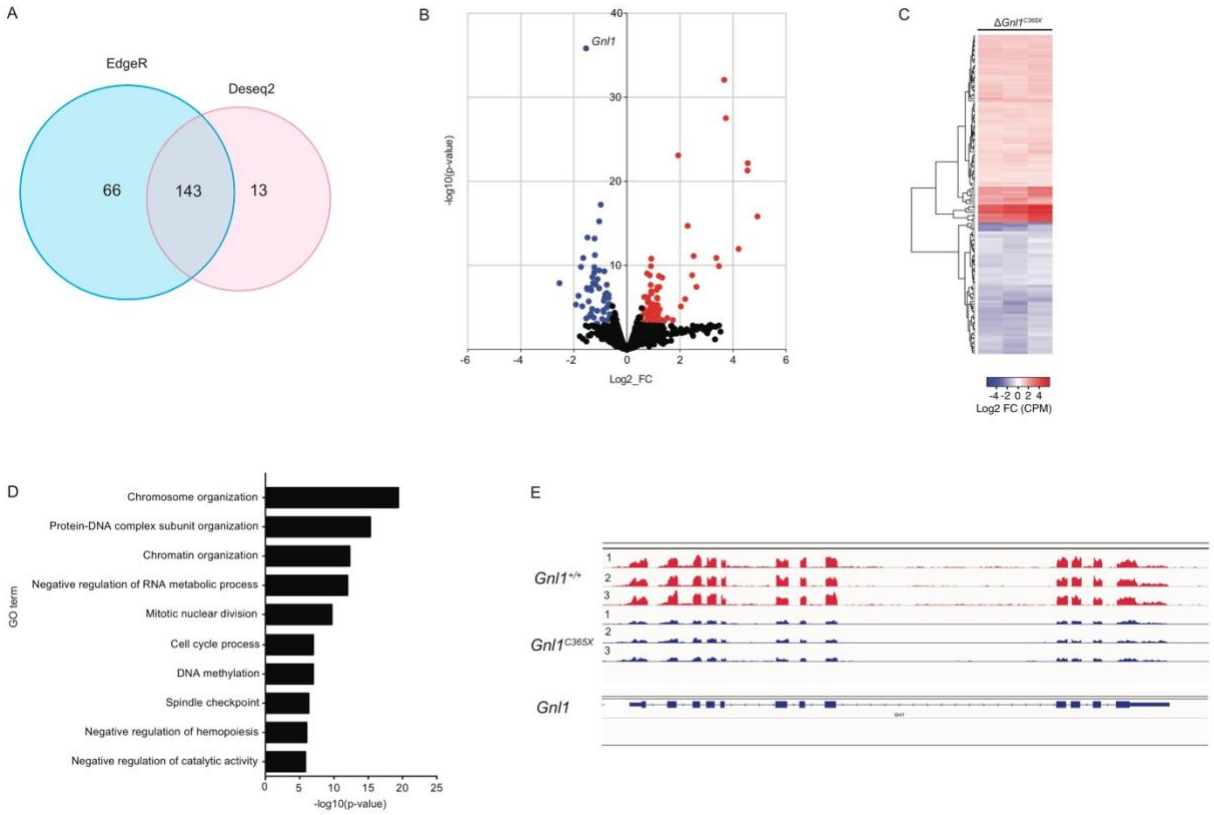

Figure 4: *Gnl1*^{C365X} NK cells differentially express 143 genes
(A) Venn diagram representing the number of significant DEGs, that met a threshold of FC > 1.5 or < -1.5 and Benjamini-Hochberg adjusted p-value < 0.05, obtained by comparing *Gnl1*^{C365X} to *Gnl1*$^{+/+}$ samples in either DESeq2 or EdgeR packages, or in both. **(B)** Volcano plot identifying upregulated DEGs in red and downregulated DEGs in blue, for DEGs that were significant in both DESeq2 and EdgeR analysis. -log10-transformed exact p-values are plotted on the y-axis and log2-transformed FC on the x-axis. All other remaining expressed genes are shown in black. **(C)** Heatmap of the 143 DEGs having met a Benjamini-Hochberg adjusted p-value of <0.05 in both EdgeR and DESeq2, and a FC > 1.5 or -1.5. Values are Log2-transformed FC (CPM of each sample divided by the mean CPM of wild-type samples). Hierarchal clustering of genes with average Euclidean distances. **(D)** 10 representative GO terms (FDR < 0.05) obtained from GO analysis on DAVID using the 143 DEG genes. **(E)** Tracks of *Gnl1* gene expression for *Gnl1*$^{+/+}$ 1-3 and *Gnl1*^{C365X} 1-3 NK cells was visualized using IGV. *Gnl1* gene with 12 exons shown below.

4.4 GSEA analysis identifies cell cycle and ribosome signatures

To further characterize the gene signatures in our set of DEGs, we performed Gene Set enrichment analysis (GSEA). Online, the Broad institute has made several libraries containing published collections of gene sets which are known to vary in response to different biological conditions (for example in response to infection, different developmental stages, different cell types) available. The goal was to compare our dataset to the library of gene sets to determine if our abundant genes matched abundant genes in these gene sets; this process is known as GSEA.

In order to perform the GSEA, all 10,857 genes which we identified to be expressed in the NK cells were used. This dataset was compared against a total of 4872 gene sets for immunological signatures; of the several enriched gene sets identified we selected the 20 most significant, of which 15 gene sets were enriched in the *Gnl1*^{C365X} NK cells and 5 genes sets were enriched in the *Gnl1*$^{+/+}$ NK cells (Fig. 5A). The enriched gene-sets in the *Gnl1*^{C365X} NK cells had signatures associated with an activation signature (group I), effector cells (group II), developing/resting cells (group III). While the gene sets enriched in *Gnl1*$^{+/+}$ NK cells also had an activated signature (group IV). For each gene set, an enrichment plot was generated. Representative gene plots for each group are illustrated in Fig. 5B. The gene rank demonstrates where all 10,871 genes fall under the curve. The genes leading the enrichment are found under the highest peak of the curve. The genes leading the enrichment in cluster/group I-III were pulled out and their expression in the *Gnl1*^{C365X} NK cells was compared to *Gnl1*$^{+/+}$. All the genes were shown to have increased expression in the mutant as compared to wild-type (Fig. 5C). However, when we compared the genes leading the enrichment to our DEGs, we noted that not all genes fell within the category. In order to gain a more global/less stringent understanding of genes, we also considered genes which were identified as differentially expressed using EdgeR or Deseq2 alone.

Next, among the signatures selected (15 in *Gnl1*^{C365X} and 5 in *Gnl1*$^{+/+}$), we pulled out the top 21 leading genes which were leading the enriched signatures in the *Gnl1*^{C365X} (Fig. 5D) and the enriched signature enriched in *Gnl1*$^{+/+}$ NK cells (Fig 5E). The vast majority of the genes leading the enrichment were among our differentially expressed genes in both wild-type and mutant NK cells. The DEGs which were enriched in mutant had increased expression when compared to wild-type and were predominantly associated with cell cycle and division (Fig. 5D). While the DEGs shown to be enriched in wild-type, had reduced expression in the mutant and the

genes are associated with processes including proliferation, stress responses and immune signalling (Fig. 5E). Therefore, using a GSEA for immunological signatures we identified a cell cycle signature driven by a significant portion of the 143 DEGs in our dataset.

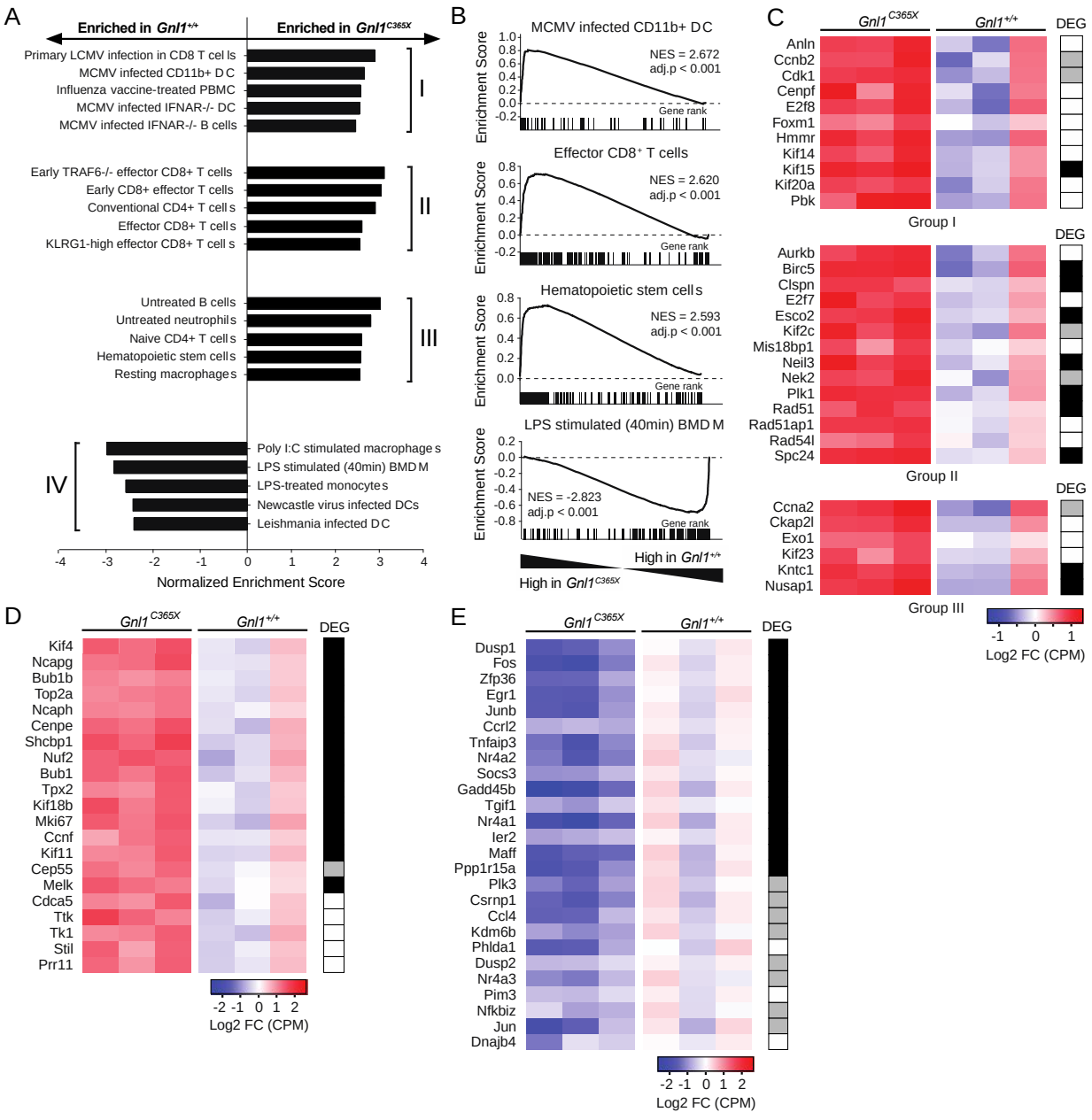

Figure 5: Cell cycle genes are leading the enrichment of immunological signatures in *Gnl1*^{C365X} NK cells

All 10,871 expressed genes in the NK cell dataset, having met a sum of 9 CPM or higher in either *Gnl1*^{C365X} or *Gnl1*$^{+/+}$ sample groups, were queried for enrichment against a gene-set collection (Immunological Signatures) in GSEA. Significantly enriched gene-sets met a FWER adjusted p-value cut-off of $p < 0.01$. **(A)** 15 enriched gene-sets in *Gnl1*^{C365X} NK cells, and 5 enriched gene-sets in *Gnl1*$^{+/+}$ NK cells, were coupled in thematic groups (I-IV) and plotted against their respective normalized enrichment scores (NES). **(B)** Enrichment plots for 3 representative gene-sets enriched in *Gnl1*^{C365X} NK cells, and 1 representative gene-set enriched in *Gnl1*$^{+/+}$ NK cells. Enrichment scores (ES) are plotted versus the rank of each gene in the gene-list (all 10,871 expressed genes). The normalized enrichment scores and the adjusted p-value are indicated for each plot. **(C-E)** Heatmaps; values represent Log2-transformed FC (CPM/mean CP of *Gnl1*$^{+/+}$ samples). The DEG column; a black cell signifies that the leading gene is among the 143 DEGs. A grey cell signifies the leading gene meets a fold change of cut-off of 1.5, and an adjusted p-value cut-off of <0.05 in either EdgeR or Deseq2, and but not in both. A white cell signifies that the leading gene is not a DEG or significant in one analysis or the other. Genes are sorted by adjusted p-value in DESeq2. **(C)** Heatmaps of the leading genes unique to each group of enriched gene sets in (correspond to groups I-III). **(D)** Heatmap of 21 leading genes that are common to groups I-III of enriched gene sets in the *Gnl1*^{C365X} samples. **(E)** Heat map of the 24 leading genes that are common to at least three enriched gene sets in *Gnl1*$^{+/+}$ (group IV).

A second GSEA was performed on the KEGG pathway collection of 186 gene sets to obtain further information on molecular pathways enriched and driven by DEGs in our data set. We identified that one signature enriched in the *Gnl1*^{C365X} NK cells was the cell cycle as depicted in the enrichment plot cell cycle (Fig. 6A). Genes leading the enrichment were selected. All genes were shown to have increased expression in the *Gnl1*^{C365X} NK cells as compared to *Gnl1*$^{+/+}$ (Fig. 6B). *Bub1b*, *Bub1* and *Plk1* were three genes leading that were among our DEGs. Bub1b and Bub1 are associated with the mitotic spindle checkpoint and Plk1-Bub1 form a kinase complex spindle checkpoint signalling (164-166). Investigating the role of these genes, we identified several studies highlighting an interplay between p53 and Bub1, Bub1b and Plk1 (167, 168). From the literature and using the p53FamTag database, we also noted that these three DEGs all contain potential binding sites for p53-mediated transcription (169, 170). To better visualize the relationship of cell cycle and p53 we mapped the DEGs identified here in a KEGG cell cycle pathway containing 112 genes associated with cell cycle (Fig 6D). As can be seen, the DEGs *Bub1*, *Bub1*, and *Plk1* (in red) were within the pathway further highlighting their role in cell cycle and the role for p53. Other genes identified as differentially expressed using EdgeR or Deseq and leading the cell cycle signatures included *CycA/Ccna2, Esp1, DP1,2* and could be associated with

the *Gnl1*^{C365X} phenotype of some are also associated with p53 (20, 171). Overall the analysis of DEGs in *Gnl1*^{C365X} NK cells show a signature suggesting aberrant cell cycle downstream of p53 activation.

Notably, a signature enriched in *Gnl1*$^{+/+}$ NK cells was the ribosome (Fig. 6A). This signature raised our interest since *Gnl1* homologs as well as human GNL1 have been shown to associate with ribosomal proteins and, under contexts of abrogated ribosome biogenesis or nucleolar, ribosomal proteins can induce p53-dependent cell cycle arrest or apoptosis. Using the less stringent approach (EdgeR or Deseq2) differentially expressed ribosomal protein (RP) genes associated with the large (RPL) or the small (RPS) subunit had reduced expression in *Gnl1*^{C365X} NK cells (Fig 6C). Among these genes *Rpl5, Rpl3, Rpl3a, Rps3* have been previously reported to result in p53-dependent cell cycle arrest and apoptosis or were shown to have responsive elements for p53 binding (170, 172-174). Although the genes leading the enrichment were not among our 143 DEGs, they were all shown to be downregulated in *Gnl1*^{C365X} NK cells (Fig 6C). Overall, the GSEA results presented here suggest that there are two potential pathways leading to NK cell death 1) cell cycle and 2) ribosomal protein genes, which both may lead to p53 activation and subsequent NK cell death ultimately leading to NK cell deficiency. Moreover, it highlights potential candidate genes which are dysregulated and therefore, contributing to the phenotype observed in *Gnl1*^{C365X} NK cells.

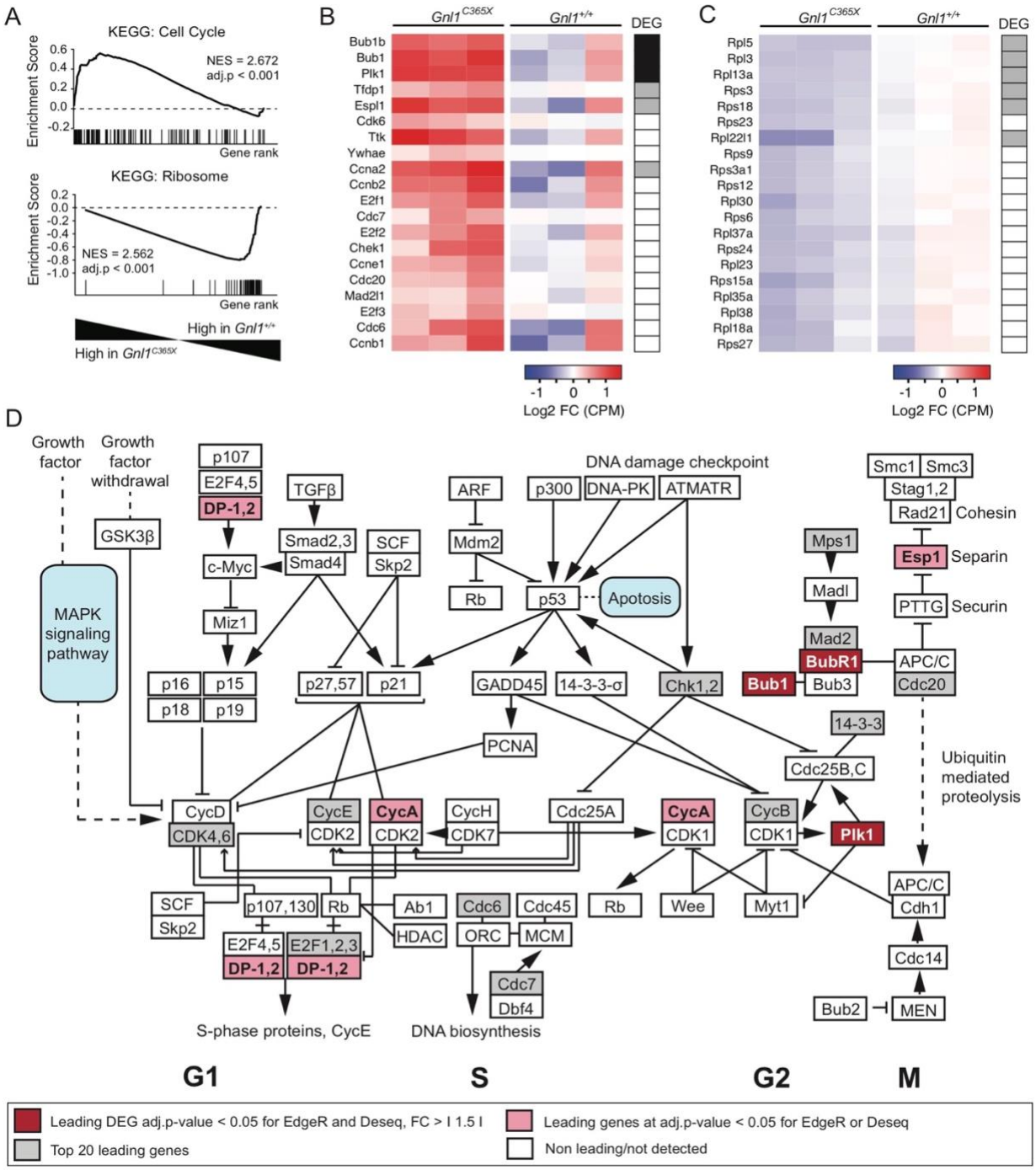
A
KEGG: Cell Cycle
Enrichment Score
NES = 2.672
adj.p < 0.001
Gene rank
KEGG: Ribosome
NES = 2.562
adj.p < 0.001
High in Gnl1+/+
High in Gnl1C365X
B
Gnl1C365X
Gnl1+/+
DEG
Bub1b
Bub1
Plk1
Tfdp1
Espl1
Cdk6
Ttk
Ywhae
Ccna2
Ccnb2
E2f1
Cdc7
E2f2
Chek1
Ccne1
Cdc20
Mad2l1
E2f3
Cdc6
Ccnb1
Log2 FC (CPM)
C
Rpl5
Rpl3
Rpl13a
Rps3
Rps18
Rps23
Rpl22l1
Rps9
Rps3a1
Rps12
Rpl30
Rps6
Rpl37a
Rps24
Rpl23
Rps15a
Rpl35a
Rpl38
Rpl18a
Rps27
D
Growth factor
Growth factor withdrawal
MAPK signaling pathway
GSK3β
p107
E2F4,5
DP-1,2
c-Myc
Miz1
TGFβ
Smad2,3
Smad4
SCF
Skp2
ARF
Mdm2
Rb
p53
Apotosis
DNA damage checkpoint
p300
DNA-PK
ATMATR
p16
p15
p18
p19
p27,57
p21
GADD45
14-3-3-σ
Chk1,2
PCNA
Smc1
Smc3
Stag1,2
Rad21
Cohesin
Mps1
Esp1
Separin
Madl
PTTG
Securin
Mad2
BubR1
Bub1
Bub3
APC/C
Cdc20
14-3-3
Cdc25B,C
Ubiquitin mediated proteolysis
CycD
CDK4,6
CycE
CDK2
CycA
CDK2
CycH
CDK7
Cdc25A
CycA
CDK1
CycB
CDK1
Plk1
SCF
Skp2
p107,130
Rb
Ab1
HDAC
Cdc6
ORC
Cdc45
MCM
Cdc7
Dbf4
Rb
Wee
Myt1
APC/C
Cdh1
Cdc14
Bub2
MEN
E2F4,5
DP-1,2
E2F1,2,3
DP-1,2
S-phase proteins, CycE
DNA biosynthesis
G1
S
G2
M
Leading DEG adj.p-value < 0.05 for EdgeR and Deseq, FC > I 1.5 I
Leading genes at adj.p-value < 0.05 for EdgeR or Deseq
Top 20 leading genes
Non leading/not detected

Figure 6: **Altered cell cycle and ribosomal protein gene expression in the KEGG pathway**
All 10,871 expressed genes in the NK cell dataset, having met a sum of 9 CPM or higher in either *Gnl1*^{C365X} or *Gnl1*$^{+/+}$ sample groups, were queried for enrichment against a gene-set collection (KEGG pathways) in GSEA. Significantly enriched gene-sets met a FWER adjusted p-value cut-off of $p < 0.01$. **(A)** Selected GSEA enrichment plots for 1 gene-set enriched in *Gnl1*^{C365X} NK cells (Cell cycle), and 1 gene-set enriched in *Gnl1*$^{+/+}$ NK cells (ribosome). Enrichment scores (ES) are plotted versus the rank of each gene in the gene-list (all 10,871 expressed genes). The normalized enrichment scores and the adjusted p-value are indicated for each plot. **(B, C)** Heatmaps; values are Log2-transformed FC (CPM/mean CP of *Gnl1*$^{+/+}$ samples). The DEG column; a black cell signifies that the leading gene is among the 143 DEGs. A grey cell signifies the leading gene meets a fold change of cut-off of 1.5, and an adjusted p-value cut-off of <0.05 in either EdgeR or Deseq2, and but not in both. **(B)** Heatmap of the 20 leading genes that drive the Cell cycle signature. **(C)** Heat map of the 20 leading genes that drive the ribosome signature. **(D)** KEGG_Cell_Cycle pathways map, representing 112 genes that are included within the KEGG_Cell_Cycle gene set (adapted from (175)).

4.5 *Gnl1*^{C365X} NK cells have increased susceptibility to p53-dependent cell death

P53 (encoded by *Trp53)* is a master regulator of numerous biological processes. P53 can function in both a transcription-dependent and in a transcription-independent manner (176). Under normal conditions, p53 is expressed at low levels in cells. However, in response to hypoxia, γ-irradiation, UV, nutrition deprivation and stress signals (such as ribosomal/nucleolar stress), p53 can be phosphorylated to produce its active form (176). Once activated it can use its transcription-dependent and independent functions to inhibit angiogenesis or induce cell cycle arrest, DNA repair and apoptosis (176).

We previously reported that there was increased apoptotic cell death in *Gnl1*^{C365X} NK cells. Moreover, using the RNA-sequencing we identified DEGs which have been associated with p53. Since apoptosis can occur through p53-dependent pathways and we see signatures and DEGs associated with p53 we wanted to further identify a link between the cell death phenotype and p53. We treated splenocytes *ex vivo* with Actinomycin (Act D). Act D activates p53 through different cell stress mechanisms based on the concentration administered. Choong et al. have shown that using 10ng/mL of Act D activates the p53 pathway via ribosomal stress by inhibiting ribosomal RNA synthesis while using 200ng/mL activates the p53 pathway via the DNA-damage pathway (177). Ultimately, treatment with Act D should activate p53 to promote cell cycle arrest and/or apoptosis. Total splenocytes were cultured with(out) 2ng/mL of IL-15 (homeostatic concentration) for 24hr and 48hr periods with varying concentrations of Act D (0, 10, 200ng/mL). Flow cytometry

was performed to assess NK cell viability (Fig. A1-B). Low concentrations of IL-15 are required to maintain NK cell viability *ex vivo*. In the absence of IL-15, NK cell viability was approximately 10-20% at 24hrs, while no viable NK cells were observed at 48 hrs which was consistent with previously reported studies demonstrating IL-15 is a cytokine crucial for NK cell survival (Fig. 7A and B). When treated with IL-15 or varying doses of Act D, no differences in cell viability were observed between wild-type and mutant NK cells at 24 hrs (Fig. 7A). However, at 48 hrs, *Gnl1*^{C365X} NK cell viability was reduced in the absence of Act D and with 10ng/mL of IL-15 (Fig. 7B). When comparing the *Gnl1*^{C365X} NK cells at 0 and 10 ng/mL of Act D in the presence of IL-15, Act D treatment further reduced viability (Fig. 7B). This reduction in viability was not observed when wild-types were compared (Fig. 7B). No differences could be reported using the 200 ng/mL of Act D at 48hrs as all cells were found to be non-viable (Fig. 7B). Taken together the data demonstrates that cell death is further promoted following p53 activation in *Gnl1*^{C365X} NK cells.

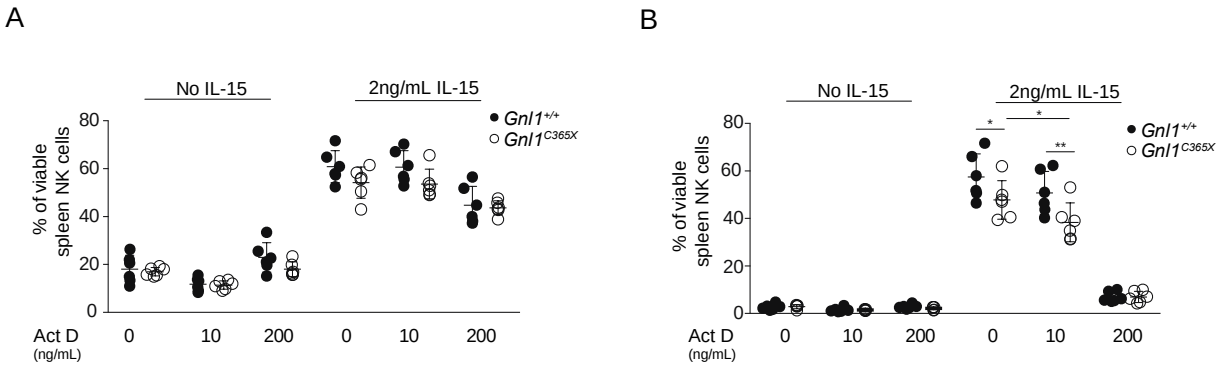

Figure 7: Actinomycin D further promotes *Gnl1*^{C365X} NK cell death via p53
(A, B) Splenocytes were cultured with or without 2ng/mL of IL-15 and varying concentrations of actinomycin D (0,10 and 200ng/mL) for **(A)** 24 hours **(B)** 48 hours at 37°C and 5% CO_2. NK cell viability was assessed using fixable viability dye. Graphic representation of results. Gating strategy is as follows; singlets (FSC-A by FSC-H), lymphocytes (FSC-A by SSC-A), NK cells ($NK1.1^+CD3^-$) and viable cells (FSC-A by Viability). Two-way ANOVA with Sidak's multiple comparisons (n= 5-6 mice/genotype). **(A, B)** All data shown as mean ± SD. P-values; *p<0.05, **p<0.01.

4.6 Knock out of *Trp53* rescues MCMV susceptibility and NK cell deficiency

In order to determine the role of p53 in mediating characteristic phenotypes of *Gnl1*^{C365X}, *Gnl1*$^{+/+}$*Trp53*$^{-/-}$ and *Gnl1*^{C365X}*Trp53*$^{-/-}$ were generated and used. Since the *Gnl1* mutation was identified in an MCMV susceptibility screen, we wanted to determine the effects of p53 on MCMV susceptibility in *Gnl1*^{C365X} mice. We performed a 14-day survival experiment. *Gnl1*$^{+/+}$, *Gnl1*^{C365X} mice, *Gnl1*$^{+/+}$*Trp53*$^{-/-}$ and *Gnl1*^{C365X}*Trp53*$^{-/-}$ mice were injected intravenously with 4,000 PFU of MCMV. As expected, *Gnl1*^{C365X} mice were susceptible to the infection however, *Gnl1*^{C365X}*Trp53*$^{-/-}$ mice were capable of overcoming the MCMV susceptibility (Fig. 8A). Another phenotype associated with *Gnl1*^{C365X} mice is their reduced weight at steady state. Here, as in the past, we observed that *Gnl1*^{C365X} mice had reduced weight compared to wild-type. However, when weighed, *Gnl1*^{C365X}*Trp53*$^{-/-}$ mice had significantly higher weight than *Gnl1*^{C365X} mice (Fig. 8B). Next, to confirm the ability of p53 to rescue the NK cell deficiency we again stained for CD49b^{+}CD3^{-}, NK1.1^{+}CD3^{-} and NKp46^{+}CD3^{-} NK cells. In terms of both proportion and cell number, we observed that the *Gnl1*^{C365X} NK cell deficiency was restored to wild-type levels in the *Gnl1*^{C365X}*Trp53*$^{-/-}$ mice (Fig. 8C-H). Moreover, we observed that the C365X mutation in *Gnl1* underlies the NK cell deficiency as *Gnl1*$^{+/+}$*Trp53*$^{-/-}$ did not portray this phenotype. The knock out was also capable of restoring the increased caspase 3 levels observed in *Gnl1*^{C365X} NK cells to wild-type levels in *Gnl1*^{C365X}*Trp53*$^{-/-}$ NK cells which suggests that the apoptosis is occurring through p53-dependent apoptosis (Fig 8I). Overall, p53-dependent mechanisms are involved in overcoming *Gnl1*^{C365X} susceptibility to MCMV, NK cell deficiency and caspase 3 expression.

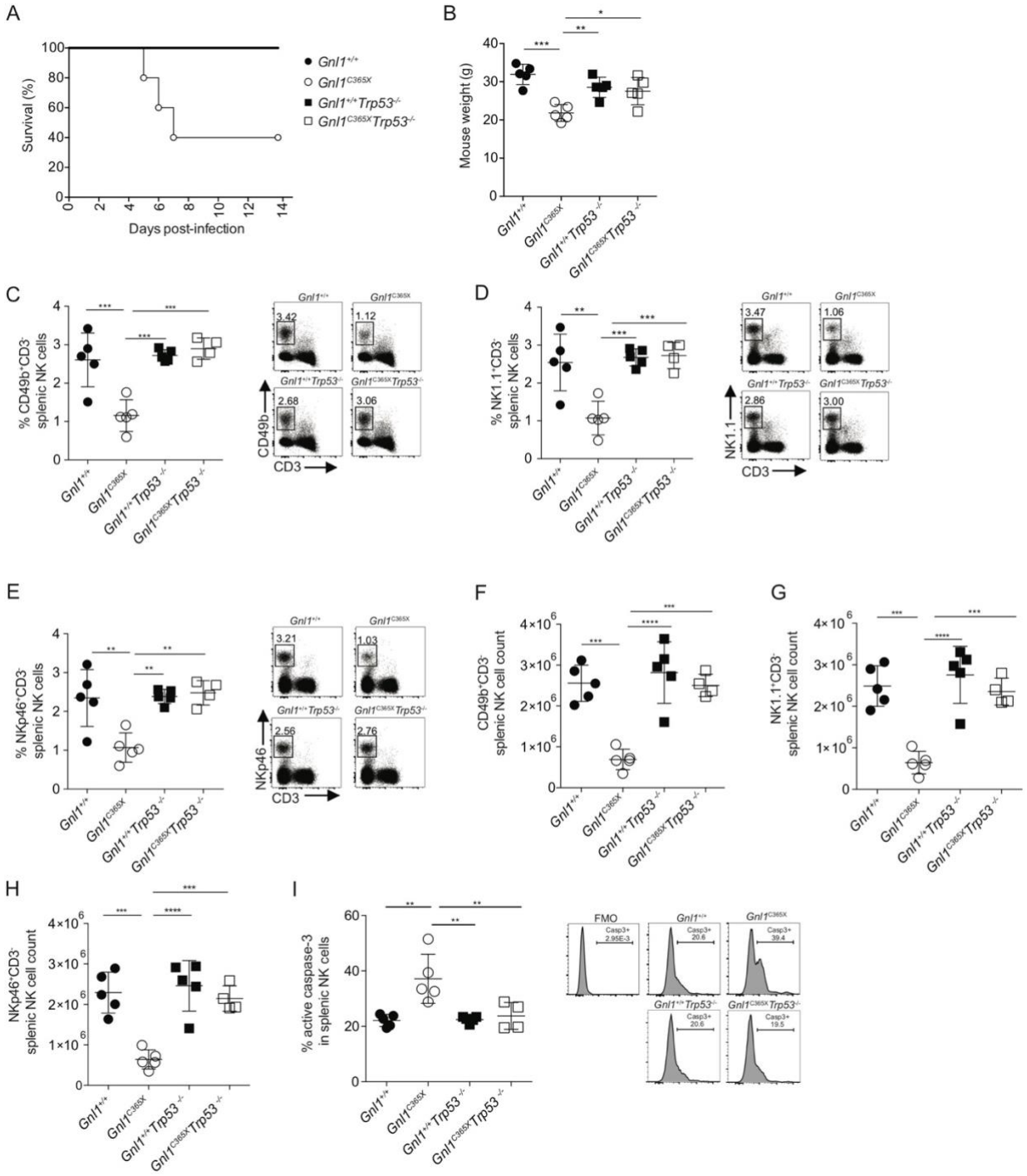
A
Survival (%)
Days post-infection
Gnl1+/+
Gnl1C365X
Gnl1+/+Trp53-/-
Gnl1C365XTrp53-/-
B
Mouse weight (g)
C
% CD49b+CD3- splenic NK cells
CD49b
CD3
3.42
1.12
2.68
3.06
D
% NK1.1+CD3- splenic NK cells
NK1.1
CD3
3.47
1.06
2.86
3.00
E
% NKp46+CD3- splenic NK cells
NKp46
CD3
3.21
1.03
2.56
2.76
F
CD49b+CD3- splenic NK cell count
G
NK1.1+CD3- splenic NK cell count
H
NKp46+CD3- splenic NK cell count
I
% active caspase-3 in splenic NK cells
FMO
Casp3+ 2.95E-3
Casp3+ 20.6
Casp3+ 39.4
Casp3+ 20.6
Casp3+ 19.5

Figure 8: *Trp53* KO overcomes MCMV susceptibility and NK cell deficiency while restoring normal caspase 3 expression in *Gnl1*^{C365X} NK cells
(A) MCMV survival graph. *Gnl1*$^{+/+}$, *Gnl1*^{C365X}, *Gnl1*$^{+/+}$*Trp53*$^{-/-}$ and *Gnl1*^{C365X}*Trp53*$^{-/-}$ mice were administered a dose of 10^4 PFU of MCMV i.v. (n = 6 - 7 mice/genotype) **(B)** Weight of male mice 11 to 12 weeks in age. **(C-E)** NK cell proportions were quantified by FACS using **(C)** CD49b$^+$CD3$^-$ **(D)** NK1.1$^+$CD3$^-$ or **(E)** NKp46$^+$CD3$^-$ staining. **(C- E)** Graphic representation and representative dot plots for each genotype are depicted for each NK cell marker. NK cell gating strategy is depicted in the appendix. **(F-H)** Total spleen NK cell count was determined using splenocyte counts and NK cell percentages from staining described in C, D, and E respectively. **(I)** Graphic and representative flow plots for the expression of active caspase 3 on NK1.1$^+$CD3$^-$ spleen cells. Fluorescence minus one (FMO) plot is also shown. **(B-I)** mean ± SD shown. Ordinary one-way ANOVA with Tukey's multiple comparisons test, n= 4-5 mice/genotype, *p<0.05, **p<0.01, ***p<0.01, ****p<0.0001.

4.7 *Trp53* KO restores NK cell maturation and receptor expression

As previously mentioned, conventional NK cells undergo a 4-stage maturational program in order to attain functional maturity. In the *Gnl1*^{C365X} mice, we identified that the NK cells were less mature than those observed in *Gnl1*$^{+/+}$ mice. In order to determine if there was a role for p53 in modulating this maturation program we performed flow cytometric analysis. As before, we observed that there was an increase in DN a decrease in DP and CD11b SP NK cell populations in *Gnl1*^{C365X} mice. The proportions were restored to wild type levels when *Trp53*$^{-/-}$ was knocked out in *Gnl1*^{C365X} mice (Fig. 9A) demonstrating a role for p53 in modulating NK cell maturation.

In order for NK cells to provide an effective cytotoxic response they require the ability to recognize activating and inhibitory ligands on target cells. Previously, in *Gnl1*^{C365X} mice, we observed that the proportion of inhibitory receptors, KLRG1 and Ly49G2 and the activating receptors NKG2D and Ly49H were reduced. To determine if there was a role for p53 in mediating their expression we monitored receptor expression in *Gnl1*^{C365X}*Trp53*$^{-/-}$ NK cells. In all cases, absence of p53 in *Gnl1*^{C365X} NK cells was capable of restoring receptor expression (Fig. 9B-D).

Moreover, a preliminary experiment identified that CD122 (IL-2Rβ/IL-15Rβ) cytokine receptor which is reduced in *Gnl1*^{C365X} mice is restored to wild-type levels in *Gnl1*^{C365X}*Trp53*$^{-/-}$ NK cells (18). Due to the importance of IL-15 for NK cells we wanted to validate this finding. As before, the MFI of CD122 was reduced in *Gnl1*^{C365X} while *Gnl1*^{C365X}*Trp53*$^{-/-}$ had a CD122 MFI similar to wild-type (Fig. 9F). Altogether the data demonstrates that while *Gnl1*^{C365X} mutation is required to alter NK cell maturation and receptor expression and p53 has a role in mediating these phenotypes.

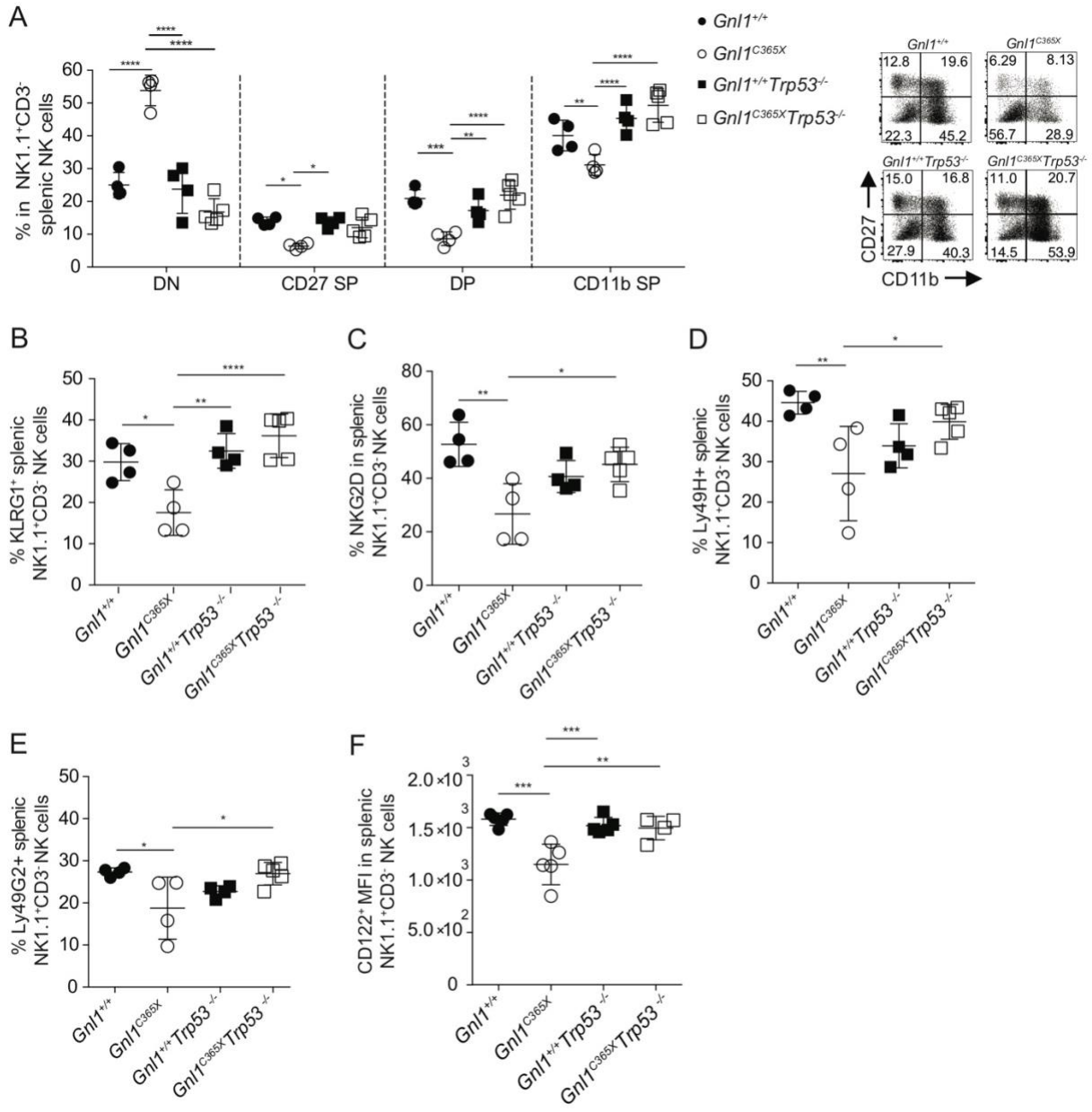

Figure 9: *Trp53* KO in *Gnl1*^{C365X} mice restores NK cell maturational program and receptor expression

Flow cytometric analysis was performed on *Gnl1*$^{+/+}$, *Gnl1*^{C365X}, *Gnl1*$^{+/+}$ *Trp53*$^{-/-}$ and *Gnl1*^{C365X} *Trp53*$^{-/-}$ splenic NK1.1^{+}CD3^{-} NK cells. **(A**) Graphic and representative flow plots of the 4-stage maturation program (CD27 and CD11b). **(B-E)** Proportion of the activating and inhibitory NK cell receptors **(B)** KLRG1, **(C)** NKG2D, **(D)** Ly49H and **(E)** Ly49G2. **(F)** CD122 mean fluorescent intensity (MFI). **(A-F)** Ordinary one-way ANOVA with Dunnett's multiple comparisons test. All data shown as mean ± SD, n = 4-5 mice/genotype, *p<0.05, **p<0.01, ***p<0.01, ****p<0.0001.

Chapter 5 – Discussion

The overall objective of this study was to identify genes and pathways which are impacted following the mutation of GNL1 that lead to the NK cell deficiency. We hypothesized that the *Gnl1*^{C365X} mutation perturbs p53 activation as well as cell cycle and ribosomal protein gene expression in NK cells. To address this hypothesis, we sought to better characterize genes that were differentially expressed between *Gnl1*$^{+/+}$ and *Gnl1*^{C365X} NK cells as well as to determine the impact of knocking out *Trp53*. In the present study we validated that *Gnl1*^{C365X} mice have an NK cell deficiency associated with increased apoptotic cell death. We developed a platform to sort NK cells and we performed RNA-sequencing in which we identified that; **(a)** there are 143 DEGs between *Gnl1*$^{+/+}$ and *Gnl1*^{C365X} NK cells, **(b) The Deseq2 and EdgeR** p-values were the most different between *Gnl1*$^{+/+}$ and *Gnl1*^{C365X} NK cells, **(c)** 1.5 fold reduced expression of *Gnl1* in the *Gnl1*^{C365X} NK cells, **(d)** using the 143 DEGs, gene ontology highlighted terms associated with cell cycle processes, **(e)** using a GSEA for immunological signatures and KEGG pathways, we identified enriched cell cycle signatures in *Gnl1*^{C365X} NK cells, **(f)** the KEGG cell cycle pathway had the DEGs *Bub1, Bub1b* and *Plk1* which are associated with p53 leading the enrichment, **(g)** the KEGG ribosome pathway was enriched in *Gnl1*$^{+/+}$ NK cells; genes leading the enrichment were ribosomal protein genes which were not among our 143 DEGs but were identified as differentially expressed using EdgeR or Deseq2 and a portion had a relationship with p53. Using Actinomycin D treatment, we showed ribosomal stress induced p53 activation resulted in a small but significant decrease in *Gnl1*^{C365X} NK cell viability. Next using *Gnl1*^{C365X}*Trp53*$^{-/-}$ mice, we demonstrated that in the absence of p53, *Gnl1*^{C365X} mice can overcome MCMV susceptibility and the NK cell deficiency. Moreover, *Trp53* KO restores caspase 3 expression, maturation and NK cell receptor expression to wild-type levels in *Gnl1*^{C365X} NK cells.

For the RNA-sequencing experiment, we specifically choose to use male mice as to omit cyclic female variation and because males, being larger, tended to have larger numbers of NK cells. However, we do not think that having used male mice skewed our results as we have not previously seen any differences in phenotype in male and female mice. In the future, we are interested in performing another RNA-sequencing using female mice. For all other experiments, the choice of using male or female mice was based on availability of mice in the colony which were within the same age range and the same sex for a given experiment.

When sorting was performed, we needed to select for viable NK cells; selecting for dying NK cells would result in the samples containing degraded RNA which would not allow us to pass the quality control step (RIN) to produce the cDNA libraries (178). However, despite this limitation, we were still able to pull out genes and signatures associated with cell cycle and the ribosome that could be inducing increased cell death.

Approximately 20 ng of RNA was used to prepare the cDNA libraries that were sequenced. In a typical RNA-sequencing experiment 400 ng of RNA is used. Due to the low amounts of RNA used, we had to perform 11 cycles of PCR enrichment instead of 8. Therefore, for us it was crucial to confirm that our data set had results within the expected ranges. A phred score of 30 has a probability of incorrect base calling of 1 in 1000 and a phred score of 40 has a probability of 1 in 10,000. With our score of 38 this demonstrated our base calling accuracy was between 99.9% and 99.99% which is relatively high. When the trimmed reads were aligned to exonic regions, the exonic rate was between 0.698 and 0.786. Overall, our data set was comparable to other studies even though it required extra amplification and it followed the guiding principles discussed in the literature (163, 178).

Bub1, *Bub1b* and *Plk1* were three DEGs leading the enrichment of the KEGG cell cycle pathway. These genes were upregulated in the *Gnl1*^{C365X} NK cells. Since we observed DEGs involved in cell cycle and we saw increased apoptotic cell death this led us to consider the role of p53. A study by McKenzie et al. demonstrated that *Plk1* is downregulated by p53 by direct repression in response to DNA damage (167). They also discuss that *Plk1* has 2 sites within its promoter which can bind p53 (167). Another study by Ando et al. found that *Plk1* binds p53 to inhibit pro-apoptotic function and transactivation activity (179). Repression of *Bub1* can activate p53-dependent premature senescence response (168). As previously mentioned, *Bub1*, *Bub1b* and *Plk1* were all identified to have p53 responsive elements using the p53FamTag database and shown to be involved in the spindle checkpoint (also known as M checkpoint) (164, 165, 170). The importance of these genes was further highlighted by the fact that GO terms specifically highlighted spindle checkpoint and mitotic nuclear division. Therefore, there is strong evidence that GNL1 is involved with the spindle checkpoint in mice. This also highlighted a potential relation between the dysregulation of these genes in *Gnl1*^{C365X} NK cells and p53.

Using an EdgeR and Deseq2 p-value cut off of less than 0.05, we identified ribosomal protein genes that were leading the enrichment of the ribosome KEGG pathway in *Gnl1*$^{+/+}$ NK cells. Moreover, we identified that these genes were downregulated in *Gnl1*^{C365X} NK cells. The ribosome is very important as it is required for the production of proteins. If the ribosome biogenesis process is altered in any way this can induce ribosomal stress which ultimately results in the activation of p53. Ribosome biogenesis consists of production of ribosomal RNA and ribosomal proteins, export of 40S and 60S ribosome, assembly and protein synthesis of the 80S (172). Ribosomal stress can be induced when this process is abrogated; free ribosomal proteins can interact with the E3 ubiquitin ligase MDM2 thereby inhibiting it from interacting with P53 and so, p53 is free to become activated (151, 172). However, ribosomal stress can also be induced when ribosomal proteins are missing as shown in several studies (172, 180-183). Since ribosomal protein transcripts seem to be downregulated in the mutant, the latter model seems to be the mechanism by which p53 is being induced. We also did see that a portion of the ribosomal protein genes did have p53 responsive elements. Moreover, a study by Šulić et al. demonstrated that in T cells, deletion of ribosomal protein S6 inhibits ribosome biogenesis which induces p53-dependent checkpoint response to inhibit cell division and increase apoptosis (180). There is a role for p21 induced block of the G1/S pathway in this study (180). In humans GNL1 has been shown to modulate the G1/S transition by interacting with RPS20 to induce phosphorylation of retinoblastoma (141). Therefore, aside from controlling M checkpoint, in mice NK cells *Gnl1* may also be modulating G1/S transition however, further studies will be required to confirm these hypotheses.

Only one studied from Collin et al. have demonstrated an association between *p53* and NK cells (184). In our study, T*rp53* knock out in *Gnl1*$^{+/+}$ mice had no impact on NK cell proportion or number. This finding was consistent with the finding from Collin et al. which showed that knocking out T*rp53* in B6 mice did not affect NK cell number (184). Our data demonstrates that the deficiency in NK cells is a consequence of the *Gnl1*^{C365X} mutation which is perturbing p53 pathways. By knocking out *Trp53*, we are able to restore the increased caspase 3 expression observed in *Gnl1*^{C365X} NK cells to wild-type levels. Initially we knew that the *Gnl1*^{C365X} NK cells were undergoing increased apoptotic cell death (18). However, here we demonstrate that apoptosis is being induced via a p53-dependent mechanism. Moreover, MCMV susceptibility observed in the *Gnl1*^{C365X} mice was overcome in *Gnl1*^{C365X}*Trp53*$^{-/-}$ mice. This can be explained by the fact that

NK cell percentages and numbers were restored to wild-type levels. In addition, it further validates our previous findings that the inability to provide protection against MCMV infection is not a result of their ability to initiate responses but rather their inability to have a strong response due to cell number.

IL-15 is essential for the production of a functional NK cell compartment (83). We previously demonstrated that the *Gnl1*^{C365X} NK cells do not effectively respond to IL-15 and undergo increased apoptosis and reduced proliferation (18). One reason why the *Gnl1*^{C365X} NK cells have reduced survival could be associated with their inability to respond to IL-15 as a result of reduced receptor expression of CD122 therefore, without CD122, IL-15 cannot efficiently signal to JAK/STAT, Ras-Raf-Mek-Erk or the mTOR pathway. In preliminary studies, we did observe reduced STAT5 and mTOR activation in the *Gnl1*^{C365X} NK cells. STAT5 signalling is known to promote transcription of cell survival and proliferative genes (83). Therefore, without efficient signalling, levels of transcription of these genes could be reduced and thus the p53-depedent cell death/cell cycle pathways can be altered. Here we validated previous findings, that KO of *Trp53* in *Gnl1*^{C365X} NK cells restore CD122 receptor expression. However, it is still an open question as to how p53 is associated with CD122 expression; it may be that p53 directly or indirectly regulates CD122 expression, but further studies are needed to address the relationship.

A small but significant decrease in NK cell viability was observed when we compared *Gnl1*^{C365X} NK cells treated with 0 ng/mL of Act D with 10ng/mL of Act D in the presence of IL-15. This finding was consistent with what we expected and with our RNA-sequencing and flow cytometry data. Only 5-6 mice were used in the study. In order to further see the effect of Act D on NK cell viability as a result of induction of p53 due to ribosomal stress, more mice would be required. Although small, we do believe that cell death is further promoted following p53 activation in *Gnl1*^{C365X} NK cells.

We have previously observed that NK development is altered in *Gnl1*^{C365X} NK cells. We have also seen that the deficiency stems all the way back to the HSCs. Therefore, to obtain a better understanding of the role of p53 it would be important to perform similar experiments using BM cells. The NK cells may be less mature in *Gnl1*^{C365X} mice because they cannot follow the normal developmental pathway, and this may be associated with p53 activation.

Our current working model is that in *Gnl1*$^{+/+}$ NK cells, the cells are growing normally; transcription of ribosomal protein genes and the assembly of functional ribosome occurs therefore, the p53 pathway (transcription dependent/independent) is not activated so normal cell cycle, proliferation and survival occurs. However, in the context of *Gnl1*^{C365X} NK cells, ribosomal transcripts are not being transcribed as efficiently therefore inducing p53-dependent checkpoint responses to promote abnormal cell cycle, proliferation and survival.

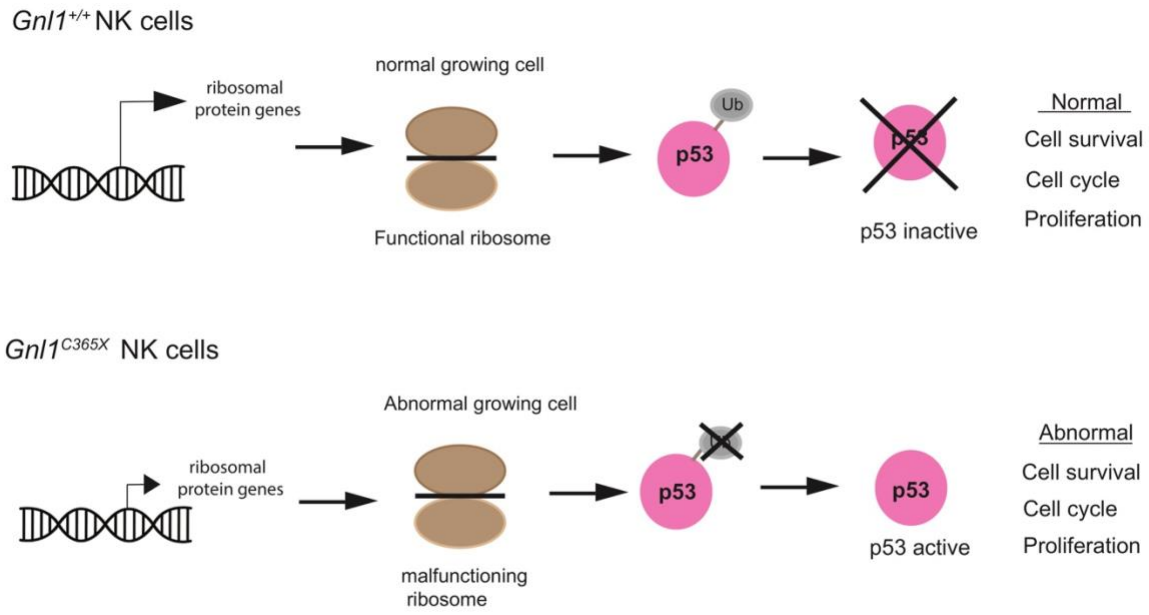

Figure 10 – Working model
Normal levels of transcription of ribosomal protein genes occurs in *Gnl1*$^{+/+}$ NK cells which allows for proper assembly and function of the ribosome. Under these circumstances p53 will remain inactive so normal cellular processes occur. In the context of *Gnl1*^{C365X} NK cells, there is reduced transcription of ribosomal protein genes therefore, there is improper assembly and function of the ribosome which induces ribosomal stress to activate p53 which induces abnormal cellular processes. References (172, 176)

Based on the work that has been done thus far, there are several future directions for the project. A study from Pelletier et al. demonstrated that when the MHC locus (locus containing *Gnl1*) is impacted on chromosome 17 in mice, it results in an NK cell deficiency in terms of both proportion and number which is what we have seen (185). This study further highlights the relationship between the mutation in *Gnl1* and the NK cell deficiency. However, to confirm that

Gnl1 is the gene resulting in the NK cell deficiency and other associated phenotypes, *Gnl1* knock out mice can be generated using CRISPR-cas9. Once generated we would need to validate (a) MCMV susceptibility, (b) NK cell deficiency, (c) maturational defects, (d) reduced receptor expression, (e) inability to proliferate, (f) increased cell death is a result of alterations in *Gnl1*/GNL1.

Further analyses using the RNA-sequencing data will be performed. Using ingenuity pathway analysis (IPA) and/or STRING, we will look for upstream regulators. We will also use the Data Browser ImmGen which contains microarray and RNA-seq data to see if we can better define the developmental stage in which $Gnl1^{C365X}$ NK cells are arrested. We will also look for databases containing p53 targets and networks in order to see if we obtain a better understanding of the relationship of our 143 DEGs and p53.

Droplet digital polymerase chain reaction (ddPCR) is a digital PCR method which will allow us to compare relative expression levels of target genes. We will use this method for several purposes. First, we will validate that *Bub1, Bub1b, Plk1* are upregulated in $Gnl1^{C365X}$ NK cells as compared to $Gnl1^{+/+}$ NK cells at steady state. It may also be of interest, to perform the ddPCR on the ribosomal protein genes *Rpl5, Rpl3, Rpl13a, Rps3, Rps18, Rpl22l1* to identify if their expression is reduced in $Gnl1^{C365X}$ NK cells as compared to $Gnl1^{+/+}$ NK cells. Since they were only identified using EdgeR or Deseq2 it would be beneficial to take sorted NK cells and stimulate them with high levels of IL-15 as done by Marçais et al. to induce the mTOR pathway which induces translation. It would also be of interest to do ddPCR on $Gnl1^{+/+}$, $Gnl1^{C365X}$, $Gnl1^{+/+}Trp53^{-/-}$, $Gnl1^{C365X}Trp53^{-/-}$ for the genes validated as differentially expressed to identify if there is a role for p53.

In order to identify if GNL1 interacts directly with the ribosome, ribosome profiling could be performed. $Gnl1^{+/+}$ and $Gnl1^{C365X}$ splenic NK cells will be sorted and then stimulated for several days with IL-15 to promote ribosome biogenesis/function. Lysates will be run on a 10-25% sucrose gradient. The gradient will be fractionated and collected while monitoring for an optical density (OD) of 254nm. Via Western blot, the expression 40S ribosomal proteins and the 60S ribosomal proteins and GNL1 will be probed and aligned to identify if GNL1 is found within the same fractions as the ribosomal proteins suggesting that the GNL1 and the ribosomal proteins are interacting. A ribosome profile depicting the small (40S) and large (60S) ribosomal subunits and

the 80S ribosome which were separated based on their Svedberg coefficients on the sucrose gradient is also generated. It would be of interest to compare the profiles of wild-type and mutant NK cells.

BioID could also be used to identify *Gnl1* binding partners. Here, *Gnl1* would be attached to a biotin-ligase which can biotinylate proteins based on proximity. This study would further our understanding about proteins and pathways which could be altered when Gnl1 harbors the C365X mutation.

Chapter 6 - Final conclusions & summary

The goal of the current study was to understand the mechanism by which mutation of GNL1 leads to an NK cell deficiency. To do so, we performed RNA-sequencing on $Gnl1^{+/+}$ and $Gnl1^{C365X}$ NK cells in which we identified 143 DEGs. Gene ontology highlighted terms associated with cell cycle processes. GSEA on KEGG pathways indicated that $Gnl1^{C365X}$ NK cells had a cell cycle signature which was being led by several genes of which *Bub1, Bub1b* and *Plk1* were among the 143 DEGs. Using a less stringent selection process, we also observed that ribosomal protein gene expression was reduced in $Gnl1^{C365X}$ NK cells. The ribosomal protein genes and the cell cycle genes were associated with p53 in other models; this prompted us to produce $Gnl1^{C365X}Trp53^{-/-}$ mice in which we observed that the mice overcame MCMV susceptibility as well as the NK cell deficiency. The mice also had restored caspase 3 and receptor expression. Therefore, here we demonstrated that the NK cells are dying via a p53-dependent apoptotic pathway. Moreover, based on the signatures we identified using the KEGG GSEAs, we propose that cell death may be occurring due to ribosomal stress which is due to reduced transcription of ribosomal protein genes. The ribosomal stress is inducing p53 activation which is ultimately resulting cell cycle blockades which are occurring at the spindle checkpoint (*Bub1, Bub1b*) as well as at the G1/S stage. The findings of this study are significant for several reasons. For one, the study allowed us to gain a further understanding of p53; a protein which is crucial in many cells but whose functions/pathways still remain unknown. Moreover, studying the *Gnl1* mutation can help reveal novel and conserved pathways important for NK cell homeostasis downstream of IL-15; understanding these pathways could serve to enhance the potential therapeutic applications of NK cells, currently pursued by several companies.

References

1. Greenberg, A. H. 1994. The origins of the NK cell, or a Canadian in King Ivan's court. *Clin Invest Med* 17: 626-631.
2. Abel, A. M., C. Yang, M. S. Thakar, and S. Malarkannan. 2018. Natural Killer Cells: Development, Maturation, and Clinical Utilization. *Front Immunol* 9: 1869.
3. Vivier, E., E. Tomasello, M. Baratin, T. Walzer, and S. Ugolini. 2008. Functions of natural killer cells. *Nat Immunol* 9: 503-510.
4. Spits, H., J. H. Bernink, and L. Lanier. 2016. NK cells and type 1 innate lymphoid cells: partners in host defense. *Nat Immunol* 17: 758-764.
5. Zhang, Y., S. Gao, J. Xia, and F. Liu. 2018. Hematopoietic Hierarchy - An Updated Roadmap. *Trends Cell Biol* 28: 976-986.
6. Sykes, S. M., and D. T. Scadden. 2013. Modeling human hematopoietic stem cell biology in the mouse. *Semin Hematol* 50: 92-100.
7. Morrison, S. J., and I. L. Weissman. 1994. The long-term repopulating subset of hematopoietic stem cells is deterministic and isolatable by phenotype. *Immunity* 1: 661-673.
8. Seita, J., and I. L. Weissman. 2010. Hematopoietic stem cell: self-renewal versus differentiation. *Wiley Interdiscip Rev Syst Biol Med* 2: 640-653.
9. Morrison, S. J., A. M. Wandycz, H. D. Hemmati, D. E. Wright, and I. L. Weissman. 1997. Identification of a lineage of multipotent hematopoietic progenitors. *Development* 124: 1929-1939.
10. Kondo, M., I. L. Weissman, and K. Akashi. 1997. Identification of clonogenic common lymphoid progenitors in mouse bone marrow. *Cell* 91: 661-672.
11. Akashi, K., D. Traver, T. Miyamoto, and I. L. Weissman. 2000. A clonogenic common myeloid progenitor that gives rise to all myeloid lineages. *Nature* 404: 193-197.
12. Goh, W., and N. D. Huntington. 2017. Regulation of Murine Natural Killer Cell Development. *Front Immunol* 8: 130.
13. Yang, Q., F. Li, C. Harly, S. Xing, L. Ye, X. Xia, H. Wang, X. Wang, S. Yu, X. Zhou, M. Cam, H. H. Xue, and A. Bhandoola. 2015. TCF-1 upregulation identifies early innate lymphoid progenitors in the bone marrow. *Nat Immunol* 16: 1044-1050.
14. Yu, X., Y. Wang, M. Deng, Y. Li, K. A. Ruhn, C. C. Zhang, and L. V. Hooper. 2014. The basic leucine zipper transcription factor NFIL3 directs the development of a common innate lymphoid cell precursor. *Elife* 3.
15. Male, V., and H. J. Brady. 2014. Transcriptional control of NK cell differentiation and function. *Curr Top Microbiol Immunol* 381: 173-187.
16. Geiger, T. L., and J. C. Sun. 2016. Development and maturation of natural killer cells. *Curr Opin Immunol* 39: 82-89.
17. Romee, R., S. E. Schneider, J. W. Leong, J. M. Chase, C. R. Keppel, R. P. Sullivan, M. A. Cooper, and T. A. Fehniger. 2012. Cytokine activation induces human memory-like NK cells. *Blood* 120: 4751-4760.
18. Leiva-Torres, G. A. 2017. Mouse chemical mutagenesis to identify new immune mechanisms against cytomegalovirus and herpres simplex virus 1 In *Human Genetics*. McGill University 1-228.

19. 1996. In *Medical Microbiology*. th, and S. Baron, eds, Galveston (TX).
20. Hitchens, M. R., and P. D. Robbins. 2003. The role of the transcription factor DP in apoptosis. *Apoptosis* 8: 461-468.
21. Tian, C., and Y. Zhang. 2016. Purification of hematopoietic stem cells from bone marrow. *Ann Hematol* 95: 543-547.
22. Leong, J. W., J. A. Wagner, A. R. Ireland, and T. A. Fehniger. 2017. Transcriptional and post-transcriptional regulation of NK cell development and function. *Clin Immunol* 177: 60-69.
23. Chiossone, L., J. Chaix, N. Fuseri, C. Roth, E. Vivier, and T. Walzer. 2009. Maturation of mouse NK cells is a 4-stage developmental program. *Blood* 113: 5488-5496.
24. Chaplin, D. D. 2010. Overview of the immune response. *J Allergy Clin Immunol* 125: S3-23.
25. Elemam, N. M., S. Hannawi, and A. A. Maghazachi. 2017. Innate Lymphoid Cells (ILCs) as Mediators of Inflammation, Release of Cytokines and Lytic Molecules. *Toxins (Basel)* 9.
26. Zhang, Y., and B. Huang. 2017. The Development and Diversity of ILCs, NK Cells and Their Relevance in Health and Diseases. *Adv Exp Med Biol* 1024: 225-244.
27. Yokoyama, W. M., D. K. Sojka, H. Peng, and Z. Tian. 2013. Tissue-resident natural killer cells. *Cold Spring Harb Symp Quant Biol* 78: 149-156.
28. Peng, H., E. Wisse, and Z. Tian. 2016. Liver natural killer cells: subsets and roles in liver immunity. *Cell Mol Immunol* 13: 328-336.
29. Nozad Charoudeh, H., Y. Tang, M. Cheng, C. M. Cilio, S. E. Jacobsen, and E. Sitnicka. 2010. Identification of an NK/T cell-restricted progenitor in adult bone marrow contributing to bone marrow- and thymic-dependent NK cells. *Blood* 116: 183-192.
30. Wu, Y., Z. Tian, and H. Wei. 2017. Developmental and Functional Control of Natural Killer Cells by Cytokines. *Front Immunol* 8: 930.
31. Ciriza, J., H. Thompson, R. Petrosian, J. O. Manilay, and M. E. Garcia-Ojeda. 2013. The migration of hematopoietic progenitors from the fetal liver to the fetal bone marrow: lessons learned and possible clinical applications. *Exp Hematol* 41: 411-423.
32. Sojka, D. K., B. Plougastel-Douglas, L. Yang, M. A. Pak-Wittel, M. N. Artyomov, Y. Ivanova, C. Zhong, J. M. Chase, P. B. Rothman, J. Yu, J. K. Riley, J. Zhu, Z. Tian, and W. M. Yokoyama. 2014. Tissue-resident natural killer (NK) cells are cell lineages distinct from thymic and conventional splenic NK cells. *Elife* 3: e01659.
33. Vosshenrich, C. A., M. E. Garcia-Ojeda, S. I. Samson-Villeger, V. Pasqualetto, L. Enault, O. Richard-Le Goff, E. Corcuff, D. Guy-Grand, B. Rocha, A. Cumano, L. Rogge, S. Ezine, and J. P. Di Santo. 2006. A thymic pathway of mouse natural killer cell development characterized by expression of GATA-3 and CD127. *Nat Immunol* 7: 1217-1224.
34. Trinchieri, G. 1989. Biology of natural killer cells. *Adv Immunol* 47: 187-376.
35. Herberman, R. B., M. E. Nunn, and D. H. Lavrin. 1975. Natural cytotoxic reactivity of mouse lymphoid cells against syngeneic acid allogeneic tumors. I. Distribution of reactivity and specificity. *Int J Cancer* 16: 216-229.
36. Kiessling, R., E. Klein, and H. Wigzell. 1975. "Natural" killer cells in the mouse. I. Cytotoxic cells with specificity for mouse Moloney leukemia cells. Specificity and distribution according to genotype. *Eur J Immunol* 5: 112-117.
37. Marcais, A., M. Marotel, S. Degouve, A. Koenig, S. Fauteux-Daniel, A. Drouillard, H. Schlums, S. Viel, L. Besson, O. Allatif, M. Blery, E. Vivier, Y. Bryceson, O. Thaunat, and T.

Walzer. 2017. High mTOR activity is a hallmark of reactive natural killer cells and amplifies early signaling through activating receptors. *Elife* 6.

38. Karre, K., H. G. Ljunggren, G. Piontek, and R. Kiessling. 1986. Selective rejection of H-2-deficient lymphoma variants suggests alternative immune defence strategy. *Nature* 319: 675-678.
39. Rahim, M. M., M. M. Tu, A. B. Mahmoud, A. Wight, E. Abou-Samra, P. D. Lima, and A. P. Makrigiannis. 2014. Ly49 receptors: innate and adaptive immune paradigms. *Front Immunol* 5: 145.
40. Liao, N. S., M. Bix, M. Zijlstra, R. Jaenisch, and D. Raulet. 1991. MHC class I deficiency: susceptibility to natural killer (NK) cells and impaired NK activity. *Science* 253: 199-202.
41. Hecht, M. L., B. Rosental, T. Horlacher, O. Hershkovitz, J. L. De Paz, C. Noti, S. Schauer, A. Porgador, and P. H. Seeberger. 2009. Natural cytotoxicity receptors NKp30, NKp44 and NKp46 bind to different heparan sulfate/heparin sequences. *J Proteome Res* 8: 712-720.
42. Farag, S. S., T. A. Fehniger, L. Ruggeri, A. Velardi, and M. A. Caligiuri. 2002. Natural killer cell receptors: new biology and insights into the graft-versus-leukemia effect. *Blood* 100: 1935-1947.
43. Gazit, R., R. Gruda, M. Elboim, T. I. Arnon, G. Katz, H. Achdout, J. Hanna, U. Qimron, G. Landau, E. Greenbaum, Z. Zakay-Rones, A. Porgador, and O. Mandelboim. 2006. Lethal influenza infection in the absence of the natural killer cell receptor gene Ncr1. *Nat Immunol* 7: 517-523.
44. Thoren, F. B., R. E. Riise, J. Ousback, M. Della Chiesa, M. Alsterholm, E. Marcenaro, S. Pesce, C. Prato, C. Cantoni, J. Bylund, L. Moretta, and A. Moretta. 2012. Human NK Cells induce neutrophil apoptosis via an NKp46- and Fas-dependent mechanism. *J Immunol* 188: 1668-1674.
45. Paust, S., H. S. Gill, B. Z. Wang, M. P. Flynn, E. A. Moseman, B. Senman, M. Szczepanik, A. Telenti, P. W. Askenase, R. W. Compans, and U. H. von Andrian. 2010. Critical role for the chemokine receptor CXCR6 in NK cell-mediated antigen-specific memory of haptens and viruses. *Nat Immunol* 11: 1127-1135.
46. Daniels, K. A., G. Devora, W. C. Lai, C. L. O'Donnell, M. Bennett, and R. M. Welsh. 2001. Murine cytomegalovirus is regulated by a discrete subset of natural killer cells reactive with monoclonal antibody to Ly49H. *J Exp Med* 194: 29-44.
47. Wende, H., M. Colonna, A. Ziegler, and A. Volz. 1999. Organization of the leukocyte receptor cluster (LRC) on human chromosome 19q13.4. *Mamm Genome* 10: 154-160.
48. Carrillo-Bustamante, P., C. Kesmir, and R. J. de Boer. 2016. The evolution of natural killer cell receptors. *Immunogenetics* 68: 3-18.
49. Braud, V. M., D. S. Allan, C. A. O'Callaghan, K. Soderstrom, A. D'Andrea, G. S. Ogg, S. Lazetic, N. T. Young, J. I. Bell, J. H. Phillips, L. L. Lanier, and A. J. McMichael. 1998. HLA-E binds to natural killer cell receptors CD94/NKG2A, B and C. *Nature* 391: 795-799.
50. Sallman, D. A., and J. Y. Djeu. 2007. Immunological Sculpting: Natural Killer Cell Receptors and Ligands. In *Cancer Immunotherapy*. Elsevier. 63-81.
51. Donatelli, S. S., and J. Y. Djeu. 2013. Immunological Sculpting: Natural Killer-Cell Receptors and Ligands. In *Cancer Immunotherapy*. Elsevier. 115-127.
52. Spear, P., M. R. Wu, M. L. Sentman, and C. L. Sentman. 2013. NKG2D ligands as therapeutic targets. *Cancer Immun* 13: 8.

53. Houchins, J. P., T. Yabe, C. McSherry, and F. H. Bach. 1991. DNA sequence analysis of NKG2, a family of related cDNA clones encoding type II integral membrane proteins on human natural killer cells. *J Exp Med* 173: 1017-1020.
54. Fogel, L. A., M. M. Sun, T. L. Geurs, L. N. Carayannopoulos, and A. R. French. 2013. Markers of nonselective and specific NK cell activation. *J Immunol* 190: 6269-6276.
55. Karlhofer, F. M., and W. M. Yokoyama. 1991. Stimulation of murine natural killer (NK) cells by a monoclonal antibody specific for the NK1.1 antigen. IL-2-activated NK cells possess additional specific stimulation pathways. *J Immunol* 146: 3662-3673.
56. Guthmann, M. D., M. Tal, and I. Pecht. 1995. A secretion inhibitory signal transduction molecule on mast cells is another C-type lectin. *Proc Natl Acad Sci U S A* 92: 9397-9401.
57. Ito, M., T. Maruyama, N. Saito, S. Koganei, K. Yamamoto, and N. Matsumoto. 2006. Killer cell lectin-like receptor G1 binds three members of the classical cadherin family to inhibit NK cell cytotoxicity. *J Exp Med* 203: 289-295.
58. Huntington, N. D., H. Tabarias, K. Fairfax, J. Brady, Y. Hayakawa, M. A. Degli-Esposti, M. J. Smyth, D. M. Tarlinton, and S. L. Nutt. 2007. NK cell maturation and peripheral homeostasis is associated with KLRG1 up-regulation. *J Immunol* 178: 4764-4770.
59. Muller-Durovic, B., A. Lanna, L. P. Covre, R. S. Mills, S. M. Henson, and A. N. Akbar. 2016. Killer Cell Lectin-like Receptor G1 Inhibits NK Cell Function through Activation of Adenosine 5'-Monophosphate-Activated Protein Kinase. *J Immunol* 197: 2891-2899.
60. Robbins, S. H., K. B. Nguyen, N. Takahashi, T. Mikayama, C. A. Biron, and L. Brossay. 2002. Cutting edge: inhibitory functions of the killer cell lectin-like receptor G1 molecule during the activation of mouse NK cells. *J Immunol* 168: 2585-2589.
61. Robbins, S. H., M. S. Tessmer, T. Mikayama, and L. Brossay. 2004. Expansion and contraction of the NK cell compartment in response to murine cytomegalovirus infection. *J Immunol* 173: 259-266.
62. Lanier, L. L. 2005. NK cell recognition. *Annu Rev Immunol* 23: 225-274.
63. He, Y., and Z. Tian. 2017. NK cell education via nonclassical MHC and non-MHC ligands. *Cell Mol Immunol* 14: 321-330.
64. Kim, S., J. Poursine-Laurent, S. M. Truscott, L. Lybarger, Y. J. Song, L. Yang, A. R. French, J. B. Sunwoo, S. Lemieux, T. H. Hansen, and W. M. Yokoyama. 2005. Licensing of natural killer cells by host major histocompatibility complex class I molecules. *Nature* 436: 709-713.
65. Belanger, S., M. M. Tu, M. M. Rahim, A. B. Mahmoud, R. Patel, L. H. Tai, A. D. Troke, B. T. Wilhelm, J. R. Landry, Q. Zhu, K. S. Tung, D. H. Raulet, and A. P. Makrigiannis. 2012. Impaired natural killer cell self-education and "missing-self" responses in Ly49-deficient mice. *Blood* 120: 592-602.
66. Lee, K. M., M. E. McNerney, S. E. Stepp, P. A. Mathew, J. D. Schatzle, M. Bennett, and V. Kumar. 2004. 2B4 acts as a non-major histocompatibility complex binding inhibitory receptor on mouse natural killer cells. *J Exp Med* 199: 1245-1254.
67. Lee, K. M., J. P. Forman, M. E. McNerney, S. Stepp, S. Kuppireddi, D. Guzior, Y. E. Latchman, M. H. Sayegh, H. Yagita, C. K. Park, S. B. Oh, C. Wulfing, J. Schatzle, P. A. Mathew, A. H. Sharpe, and V. Kumar. 2006. Requirement of homotypic NK-cell interactions through 2B4(CD244)/CD48 in the generation of NK effector functions. *Blood* 107: 3181-3188.

68. Brandstadter, J. D., and Y. Yang. 2011. Natural killer cell responses to viral infection. *J Innate Immun* 3: 274-279.
69. Andoniou, C. E., J. D. Coudert, and M. A. Degli-Esposti. 2008. Killers and beyond: NK-cell-mediated control of immune responses. *Eur J Immunol* 38: 2938-2942.
70. Thomas, R., and X. Yang. 2016. NK-DC Crosstalk in Immunity to Microbial Infection. *J Immunol Res* 2016: 6374379.
71. Moretta, L., G. Ferlazzo, C. Bottino, M. Vitale, D. Pende, M. C. Mingari, and A. Moretta. 2006. Effector and regulatory events during natural killer-dendritic cell interactions. *Immunol Rev* 214: 219-228.
72. Lam, V. C., and L. L. Lanier. 2017. NK cells in host responses to viral infections. *Curr Opin Immunol* 44: 43-51.
73. Walzer, T., M. Dalod, S. H. Robbins, L. Zitvogel, and E. Vivier. 2005. Natural-killer cells and dendritic cells: "l'union fait la force". *Blood* 106: 2252-2258.
74. Biron, C. A., K. B. Nguyen, G. C. Pien, L. P. Cousens, and T. P. Salazar-Mather. 1999. Natural killer cells in antiviral defense: function and regulation by innate cytokines. *Annu Rev Immunol* 17: 189-220.
75. Lucas, M., W. Schachterle, K. Oberle, P. Aichele, and A. Diefenbach. 2007. Dendritic cells prime natural killer cells by trans-presenting interleukin 15. *Immunity* 26: 503-517.
76. Zanoni, I., R. Spreafico, C. Bodio, M. Di Gioia, C. Cigni, A. Broggi, T. Gorletta, M. Caccia, G. Chirico, L. Sironi, M. Collini, M. P. Colombo, N. Garbi, and F. Granucci. 2013. IL-15 cis presentation is required for optimal NK cell activation in lipopolysaccharide-mediated inflammatory conditions. *Cell Rep* 4: 1235-1249.
77. Rosales, C. 2018. Neutrophil: A Cell with Many Roles in Inflammation or Several Cell Types? *Front Physiol* 9: 113.
78. Ermert, D., A. Zychlinsky, and C. Urban. 2009. Fungal and bacterial killing by neutrophils. *Methods Mol Biol* 470: 293-312.
79. Jaeger, B. N., J. Donadieu, C. Cognet, C. Bernat, D. Ordonez-Rueda, V. Barlogis, N. Mahlaoui, A. Fenis, E. Narni-Mancinelli, B. Beaupain, C. Bellanne-Chantelot, M. Bajenoff, B. Malissen, M. Malissen, E. Vivier, and S. Ugolini. 2012. Neutrophil depletion impairs natural killer cell maturation, function, and homeostasis. *J Exp Med* 209: 565-580.
80. Riise, R. E., E. Bernson, J. Aurelius, A. Martner, S. Pesce, M. Della Chiesa, E. Marcenaro, J. Bylund, K. Hellstrand, L. Moretta, A. Moretta, and F. B. Thoren. 2015. TLR-Stimulated Neutrophils Instruct NK Cells To Trigger Dendritic Cell Maturation and Promote Adaptive T Cell Responses. *J Immunol* 195: 1121-1128.
81. Amano, K., M. Hirayama, E. Azuma, S. Iwamoto, Y. Keida, and Y. Komada. 2015. Neutrophils induced licensing of natural killer cells. *Mediators Inflamm* 2015: 747680.
82. Pliyev, B. K., M. V. Kalintseva, S. V. Abdulaeva, K. N. Yarygin, and V. G. Savchenko. 2014. Neutrophil microparticles modulate cytokine production by natural killer cells. *Cytokine* 65: 126-129.
83. Zwirner, N. W., and C. I. Domaica. 2010. Cytokine regulation of natural killer cell effector functions. *Biofactors* 36: 274-288.
84. Ohteki, T., S. Ho, H. Suzuki, T. W. Mak, and P. S. Ohashi. 1997. Role for IL-15/IL-15 receptor beta-chain in natural killer 1.1+ T cell receptor-alpha beta+ cell development. *J Immunol* 159: 5931-5935.

85. Suzuki, H., G. S. Duncan, H. Takimoto, and T. W. Mak. 1997. Abnormal development of intestinal intraepithelial lymphocytes and peripheral natural killer cells in mice lacking the IL-2 receptor beta chain. *J Exp Med* 185: 499-505.
86. DiSanto, J. P., W. Muller, D. Guy-Grand, A. Fischer, and K. Rajewsky. 1995. Lymphoid development in mice with a targeted deletion of the interleukin 2 receptor gamma chain. *Proc Natl Acad Sci U S A* 92: 377-381.
87. Cao, X., E. W. Shores, J. Hu-Li, M. R. Anver, B. L. Kelsall, S. M. Russell, J. Drago, M. Noguchi, A. Grinberg, E. T. Bloom, and et al. 1995. Defective lymphoid development in mice lacking expression of the common cytokine receptor gamma chain. *Immunity* 2: 223-238.
88. Kennedy, M. K., M. Glaccum, S. N. Brown, E. A. Butz, J. L. Viney, M. Embers, N. Matsuki, K. Charrier, L. Sedger, C. R. Willis, K. Brasel, P. J. Morrissey, K. Stocking, J. C. Schuh, S. Joyce, and J. J. Peschon. 2000. Reversible defects in natural killer and memory CD8 T cell lineages in interleukin 15-deficient mice. *J Exp Med* 191: 771-780.
89. Lodolce, J. P., D. L. Boone, S. Chai, R. E. Swain, T. Dassopoulos, S. Trettin, and A. Ma. 1998. IL-15 receptor maintains lymphoid homeostasis by supporting lymphocyte homing and proliferation. *Immunity* 9: 669-676.
90. Cooper, M. A., J. E. Bush, T. A. Fehniger, J. B. VanDeusen, R. E. Waite, Y. Liu, H. L. Aguila, and M. A. Caligiuri. 2002. In vivo evidence for a dependence on interleukin 15 for survival of natural killer cells. *Blood* 100: 3633-3638.
91. Dubois, S., H. J. Patel, M. Zhang, T. A. Waldmann, and J. R. Muller. 2008. Preassociation of IL-15 with IL-15R alpha-IgG1-Fc enhances its activity on proliferation of NK and CD8+/CD44high T cells and its antitumor action. *J Immunol* 180: 2099-2106.
92. Bamford, R. N., A. J. Grant, J. D. Burton, C. Peters, G. Kurys, C. K. Goldman, J. Brennan, E. Roessler, and T. A. Waldmann. 1994. The interleukin (IL) 2 receptor beta chain is shared by IL-2 and a cytokine, provisionally designated IL-T, that stimulates T-cell proliferation and the induction of lymphokine-activated killer cells. *Proc Natl Acad Sci U S A* 91: 4940-4944.
93. Waldmann, T. A. 2015. The shared and contrasting roles of IL2 and IL15 in the life and death of normal and neoplastic lymphocytes: implications for cancer therapy. *Cancer Immunol Res* 3: 219-227.
94. Giri, J. G., S. Kumaki, M. Ahdieh, D. J. Friend, A. Loomis, K. Shanebeck, R. DuBose, D. Cosman, L. S. Park, and D. M. Anderson. 1995. Identification and cloning of a novel IL-15 binding protein that is structurally related to the alpha chain of the IL-2 receptor. *EMBO J* 14: 3654-3663.
95. Witalisz-Siepracka, A., K. Klein, D. Prinz, N. Leidenfrost, G. Schabbauer, A. Dohnal, and V. Sexl. 2018. Loss of JAK1 Drives Innate Immune Deficiency. *Front Immunol* 9: 3108.
96. Shuai, K., and B. Liu. 2003. Regulation of JAK-STAT signalling in the immune system. *Nat Rev Immunol* 3: 900-911.
97. Eckelhart, E., W. Warsch, E. Zebedin, O. Simma, D. Stoiber, T. Kolbe, T. Rulicke, M. Mueller, E. Casanova, and V. Sexl. 2011. A novel Ncr1-Cre mouse reveals the essential role of STAT5 for NK-cell survival and development. *Blood* 117: 1565-1573.
98. Sathe, P., R. B. Delconte, F. Souza-Fonseca-Guimaraes, C. Seillet, M. Chopin, C. J. Vandenberg, L. C. Rankin, L. A. Mielke, I. Vikstrom, T. B. Kolesnik, S. E. Nicholson, E. Vivier, M. J. Smyth, S. L. Nutt, S. P. Glaser, A. Strasser, G. T. Belz, S. Carotta, and N. D. Huntington.

2014. Innate immunodeficiency following genetic ablation of Mcl1 in natural killer cells. *Nat Commun* 5: 4539.

99. Bernasconi, A., R. Marino, A. Ribas, J. Rossi, M. Ciaccio, M. Oleastro, A. Ornani, R. Paz, M. A. Rivarola, M. Zelazko, and A. Belgorosky. 2006. Characterization of immunodeficiency in a patient with growth hormone insensitivity secondary to a novel STAT5b gene mutation. *Pediatrics* 118: e1584-1592.
100. Brantley, E. C., and E. N. Benveniste. 2008. Signal transducer and activator of transcription-3: a molecular hub for signaling pathways in gliomas. *Mol Cancer Res* 6: 675-684.
101. Wortzel, I., and R. Seger. 2011. The ERK Cascade: Distinct Functions within Various Subcellular Organelles. *Genes Cancer* 2: 195-209.
102. Huntington, N. D., H. Puthalakath, P. Gunn, E. Naik, E. M. Michalak, M. J. Smyth, H. Tabarias, M. A. Degli-Esposti, G. Dewson, S. N. Willis, N. Motoyama, D. C. Huang, S. L. Nutt, D. M. Tarlinton, and A. Strasser. 2007. Interleukin 15-mediated survival of natural killer cells is determined by interactions among Bim, Noxa and Mcl-1. *Nat Immunol* 8: 856-863.
103. Adunyah, S. E., B. J. Wheeler, and R. S. Cooper. 1997. Evidence for the involvement of LCK and MAP kinase (ERK-1) in the signal transduction mechanism of interleukin-15. *Biochem Biophys Res Commun* 232: 754-758.
104. Yu, T. K., E. G. Caudell, C. Smid, and E. A. Grimm. 2000. IL-2 activation of NK cells: involvement of MKK1/2/ERK but not p38 kinase pathway. *J Immunol* 164: 6244-6251.
105. Meresse, B., Z. Chen, C. Ciszewski, M. Tretiakova, G. Bhagat, T. N. Krausz, D. H. Raulet, L. L. Lanier, V. Groh, T. Spies, E. C. Ebert, P. H. Green, and B. Jabri. 2004. Coordinated induction by IL15 of a TCR-independent NKG2D signaling pathway converts CTL into lymphokine-activated killer cells in celiac disease. *Immunity* 21: 357-366.
106. Marcais, A., J. Cherfils-Vicini, C. Viant, S. Degouve, S. Viel, A. Fenis, J. Rabilloud, K. Mayol, A. Tavares, J. Bienvenu, Y. G. Gangloff, E. Gilson, E. Vivier, and T. Walzer. 2014. The metabolic checkpoint kinase mTOR is essential for IL-15 signaling during the development and activation of NK cells. *Nat Immunol* 15: 749-757.
107. Sabatini, D. M. 2017. Twenty-five years of mTOR: Uncovering the link from nutrients to growth. *Proc Natl Acad Sci U S A* 114: 11818-11825.
108. Land, S. C., and A. R. Tee. 2007. Hypoxia-inducible factor 1alpha is regulated by the mammalian target of rapamycin (mTOR) via an mTOR signaling motif. *J Biol Chem* 282: 20534-20543.
109. Laplante, M., and D. M. Sabatini. 2009. An emerging role of mTOR in lipid biosynthesis. *Curr Biol* 19: R1046-1052.
110. Jacinto, E., R. Loewith, A. Schmidt, S. Lin, M. A. Ruegg, A. Hall, and M. N. Hall. 2004. Mammalian TOR complex 2 controls the actin cytoskeleton and is rapamycin insensitive. *Nat Cell Biol* 6: 1122-1128.
111. Viel, S., A. Marcais, F. S. Guimaraes, R. Loftus, J. Rabilloud, M. Grau, S. Degouve, S. Djebali, A. Sanlaville, E. Charrier, J. Bienvenu, J. C. Marie, C. Caux, J. Marvel, L. Town, N. D. Huntington, L. Bartholin, D. Finlay, M. J. Smyth, and T. Walzer. 2016. TGF-beta inhibits the activation and functions of NK cells by repressing the mTOR pathway. *Sci Signal* 9: ra19.

112. Rautela, J., F. Souza-Fonseca-Guimaraes, S. Hediyeh-Zadeh, R. B. Delconte, M. J. Davis, and N. D. Huntington. 2018. Molecular insight into targeting the NK cell immune response to cancer. *Immunol Cell Biol* 96: 477-484.
113. Gotthardt, D., and V. Sexl. 2016. STATs in NK-Cells: The Good, the Bad, and the Ugly. *Front Immunol* 7: 694.
114. Ali, A. K., N. Nandagopal, and S. H. Lee. 2015. IL-15-PI3K-AKT-mTOR: A Critical Pathway in the Life Journey of Natural Killer Cells. *Front Immunol* 6: 355.
115. Mebratu, Y., and Y. Tesfaigzi. 2009. How ERK1/2 activation controls cell proliferation and cell death: Is subcellular localization the answer? *Cell Cycle* 8: 1168-1175.
116. Osinska, I., K. Popko, and U. Demkow. 2014. Perforin: an important player in immune response. *Cent Eur J Immunol* 39: 109-115.
117. Topham, N. J., and E. W. Hewitt. 2009. Natural killer cell cytotoxicity: how do they pull the trigger? *Immunology* 128: 7-15.
118. Katz, P., A. M. Zaytoun, and J. H. Lee, Jr. 1982. Mechanisms of human cell-mediated cytotoxicity. III. Dependence of natural killing on microtubule and microfilament integrity. *J Immunol* 129: 2816-2825.
119. Banerjee, P. P., R. Pandey, R. Zheng, M. M. Suhoski, L. Monaco-Shawver, and J. S. Orange. 2007. Cdc42-interacting protein-4 functionally links actin and microtubule networks at the cytolytic NK cell immunological synapse. *J Exp Med* 204: 2305-2320.
120. Law, R. H., N. Lukoyanova, I. Voskoboinik, T. T. Caradoc-Davies, K. Baran, M. A. Dunstone, M. E. D'Angelo, E. V. Orlova, F. Coulibaly, S. Verschoor, K. A. Browne, A. Ciccone, M. J. Kuiper, P. I. Bird, J. A. Trapani, H. R. Saibil, and J. C. Whisstock. 2010. The structural basis for membrane binding and pore formation by lymphocyte perforin. *Nature* 468: 447-451.
121. Bots, M., and J. P. Medema. 2006. Granzymes at a glance. *J Cell Sci* 119: 5011-5014.
122. Waterhouse, N. J., K. A. Sedelies, and J. A. Trapani. 2006. Role of Bid-induced mitochondrial outer membrane permeabilization in granzyme B-induced apoptosis. *Immunol Cell Biol* 84: 72-78.
123. Schuster, I. S., J. D. Coudert, C. E. Andoniou, and M. A. Degli-Esposti. 2016. "Natural Regulators": NK Cells as Modulators of T Cell Immunity. *Front Immunol* 7: 235.
124. Martin-Fontecha, A., L. L. Thomsen, S. Brett, C. Gerard, M. Lipp, A. Lanzavecchia, and F. Sallusto. 2004. Induced recruitment of NK cells to lymph nodes provides IFN-gamma for T(H)1 priming. *Nat Immunol* 5: 1260-1265.
125. Costantini, C., A. Micheletti, F. Calzetti, O. Perbellini, G. Pizzolo, and M. A. Cassatella. 2010. Neutrophil activation and survival are modulated by interaction with NK cells. *Int Immunol* 22: 827-838.
126. Robertson, M. J. 2002. Role of chemokines in the biology of natural killer cells. *J Leukoc Biol* 71: 173-183.
127. O'Sullivan, T. E., J. C. Sun, and L. L. Lanier. 2015. Natural Killer Cell Memory. *Immunity* 43: 634-645.
128. Sun, J. C., J. N. Beilke, and L. L. Lanier. 2009. Adaptive immune features of natural killer cells. *Nature* 457: 557-561.
129. Sun, J. C., J. N. Beilke, and L. L. Lanier. 2010. Immune memory redefined: characterizing the longevity of natural killer cells. *Immunol Rev* 236: 83-94.

130. Lemus, R., and M. H. Karol. 2008. Conjugation of haptens. *Methods Mol Med* 138: 167-182.
131. O'Leary, J. G., M. Goodarzi, D. L. Drayton, and U. H. von Andrian. 2006. T cell- and B cell-independent adaptive immunity mediated by natural killer cells. *Nat Immunol* 7: 507-516.
132. van den Boorn, J. G., C. Jakobs, C. Hagen, M. Renn, R. M. Luiten, C. J. Melief, T. Tuting, N. Garbi, G. Hartmann, and V. Hornung. 2016. Inflammasome-Dependent Induction of Adaptive NK Cell Memory. *Immunity* 44: 1406-1421.
133. Cooper, M. A., J. M. Elliott, P. A. Keyel, L. Yang, J. A. Carrero, and W. M. Yokoyama. 2009. Cytokine-induced memory-like natural killer cells. *Proc Natl Acad Sci U S A* 106: 1915-1919.
134. van Helden, M. J., D. M. Zaiss, and A. J. Sijts. 2012. CCR2 defines a distinct population of NK cells and mediates their migration during influenza virus infection in mice. *PLoS One* 7: e52027.
135. Gupta, M., and M. Shorman. 2018. Cytomegalovirus. In *StatPearls*, Treasure Island (FL).
136. Smith, L. M., G. R. Shellam, and A. J. Redwood. 2006. Genes of murine cytomegalovirus exist as a number of distinct genotypes. *Virology* 352: 450-465.
137. Mitrovic, M., J. Arapovic, S. Jordan, N. Fodil-Cornu, S. Ebert, S. M. Vidal, A. Krmpotic, M. J. Reddehase, and S. Jonjic. 2012. The NK cell response to mouse cytomegalovirus infection affects the level and kinetics of the early CD8(+) T-cell response. *J Virol* 86: 2165-2175.
138. Sumaria, N., S. L. van Dommelen, C. E. Andoniou, M. J. Smyth, A. A. Scalzo, and M. A. Degli-Esposti. 2009. The roles of interferon-gamma and perforin in antiviral immunity in mice that differ in genetically determined NK-cell-mediated antiviral activity. *Immunol Cell Biol* 87: 559-566.
139. Dokun, A. O., S. Kim, H. R. Smith, H. S. Kang, D. T. Chu, and W. M. Yokoyama. 2001. Specific and nonspecific NK cell activation during virus infection. *Nat Immunol* 2: 951-956.
140. Nguyen, K. B., T. P. Salazar-Mather, M. Y. Dalod, J. B. Van Deusen, X. Q. Wei, F. Y. Liew, M. A. Caligiuri, J. E. Durbin, and C. A. Biron. 2002. Coordinated and distinct roles for IFN-alpha beta, IL-12, and IL-15 regulation of NK cell responses to viral infection. *J Immunol* 169: 4279-4287.
141. Krishnan, R., N. Boddapati, and S. Mahalingam. 2018. Interplay between human nucleolar GNL1 and RPS20 is critical to modulate cell proliferation. *Sci Rep* 8: 11421.
142. Reynaud, E. G., M. A. Andrade, F. Bonneau, T. B. Ly, M. Knop, K. Scheffzek, and R. Pepperkok. 2005. Human Lsg1 defines a family of essential GTPases that correlates with the evolution of compartmentalization. *BMC Biol* 3: 21.
143. Mier, P., A. J. Perez-Pulido, E. G. Reynaud, and M. A. Andrade-Navarro. 2017. Reading the Evolution of Compartmentalization in the Ribosome Assembly Toolbox: The YRG Protein Family. *PLoS One* 12: e0169750.
144. Anand, B., S. K. Verma, and B. Prakash. 2006. Structural stabilization of GTP-binding domains in circularly permuted GTPases: implications for RNA binding. *Nucleic Acids Res* 34: 2196-2205.
145. Thomson, E., S. Ferreira-Cerca, and E. Hurt. 2013. Eukaryotic ribosome biogenesis at a glance. *J Cell Sci* 126: 4815-4821.

146. Bursac, S., M. C. Brdovcak, G. Donati, and S. Volarevic. 2014. Activation of the tumor suppressor p53 upon impairment of ribosome biogenesis. *Biochim Biophys Acta* 1842: 817-830.
147. Morgado-Palacin, L., S. Llanos, and M. Serrano. 2012. Ribosomal stress induces L11- and p53-dependent apoptosis in mouse pluripotent stem cells. *Cell Cycle* 11: 503-510.
148. Chen, J. 2016. The Cell-Cycle Arrest and Apoptotic Functions of p53 in Tumor Initiation and Progression. *Cold Spring Harb Perspect Med* 6: a026104.
149. Achila, D., M. Gulati, N. Jain, and R. A. Britton. 2012. Biochemical characterization of ribosome assembly GTPase RbgA in Bacillus subtilis. *J Biol Chem* 287: 8417-8423.
150. Hedges, J., M. West, and A. W. Johnson. 2005. Release of the export adapter, Nmd3p, from the 60S ribosomal subunit requires Rpl10p and the cytoplasmic GTPase Lsg1p. *EMBO J* 24: 567-579.
151. Meng, L., J. K. Hsu, and R. Y. Tsai. 2011. GNL3L depletion destabilizes MDM2 and induces p53-dependent G2/M arrest. *Oncogene* 30: 1716-1726.
152. Paridaen, J. T., E. Janson, K. H. Utami, T. C. Pereboom, P. B. Essers, C. van Rooijen, D. Zivkovic, and A. W. MacInnes. 2011. The nucleolar GTP-binding proteins Gnl2 and nucleostemin are required for retinal neurogenesis in developing zebrafish. *Dev Biol* 355: 286-301.
153. Pyzik, M., B. Charbonneau, E. M. Gendron-Pontbriand, M. Babic, A. Krmpotic, S. Jonjic, and S. M. Vidal. 2011. Distinct MHC class I-dependent NK cell-activating receptors control cytomegalovirus infection in different mouse strains. *J Exp Med* 208: 1105-1117.
154. Quatrini, L., E. Wieduwild, B. Escaliere, J. Filtjens, L. Chasson, C. Laprie, E. Vivier, and S. Ugolini. 2018. Endogenous glucocorticoids control host resistance to viral infection through the tissue-specific regulation of PD-1 expression on NK cells. *Nat Immunol* 19: 954-962.
155. Huang da, W., B. T. Sherman, and R. A. Lempicki. 2009. Systematic and integrative analysis of large gene lists using DAVID bioinformatics resources. *Nat Protoc* 4: 44-57.
156. Huang da, W., B. T. Sherman, and R. A. Lempicki. 2009. Bioinformatics enrichment tools: paths toward the comprehensive functional analysis of large gene lists. *Nucleic Acids Res* 37: 1-13.
157. Subramanian, A., P. Tamayo, V. K. Mootha, S. Mukherjee, B. L. Ebert, M. A. Gillette, A. Paulovich, S. L. Pomeroy, T. R. Golub, E. S. Lander, and J. P. Mesirov. 2005. Gene set enrichment analysis: a knowledge-based approach for interpreting genome-wide expression profiles. *Proc Natl Acad Sci U S A* 102: 15545-15550.
158. Mootha, V. K., C. M. Lindgren, K. F. Eriksson, A. Subramanian, S. Sihag, J. Lehar, P. Puigserver, E. Carlsson, M. Ridderstrale, E. Laurila, N. Houstis, M. J. Daly, N. Patterson, J. P. Mesirov, T. R. Golub, P. Tamayo, B. Spiegelman, E. S. Lander, J. N. Hirschhorn, D. Altshuler, and L. C. Groop. 2003. PGC-1alpha-responsive genes involved in oxidative phosphorylation are coordinately downregulated in human diabetes. *Nat Genet* 34: 267-273.
159. Robinson, J. T., H. Thorvaldsdottir, W. Winckler, M. Guttman, E. S. Lander, G. Getz, and J. P. Mesirov. 2011. Integrative genomics viewer. *Nat Biotechnol* 29: 24-26.

160. Thorvaldsdottir, H., J. T. Robinson, and J. P. Mesirov. 2013. Integrative Genomics Viewer (IGV): high-performance genomics data visualization and exploration. *Brief Bioinform* 14: 178-192.
161. Robinson, J. T., H. Thorvaldsdottir, A. M. Wenger, A. Zehir, and J. P. Mesirov. 2017. Variant Review with the Integrative Genomics Viewer. *Cancer Res* 77: e31-e34.
162. Jiao, Y., N. D. Huntington, G. T. Belz, and C. Seillet. 2016. Type 1 Innate Lymphoid Cell Biology: Lessons Learnt from Natural Killer Cells. *Front Immunol* 7: 426.
163. Conesa, A., P. Madrigal, S. Tarazona, D. Gomez-Cabrero, A. Cervera, A. McPherson, M. W. Szczesniak, D. J. Gaffney, L. L. Elo, X. Zhang, and A. Mortazavi. 2016. A survey of best practices for RNA-seq data analysis. *Genome Biol* 17: 13.
164. Jia, L., B. Li, and H. Yu. 2016. The Bub1-Plk1 kinase complex promotes spindle checkpoint signalling through Cdc20 phosphorylation. *Nat Commun* 7: 10818.
165. Meraldi, P., and P. K. Sorger. 2005. A dual role for Bub1 in the spindle checkpoint and chromosome congression. *EMBO J* 24: 1621-1633.
166. Overlack, K., I. Primorac, M. Vleugel, V. Krenn, S. Maffini, I. Hoffmann, G. J. Kops, and A. Musacchio. 2015. A molecular basis for the differential roles of Bub1 and BubR1 in the spindle assembly checkpoint. *Elife* 4: e05269.
167. McKenzie, L., S. King, L. Marcar, S. Nicol, S. S. Dias, K. Schumm, P. Robertson, J. C. Bourdon, N. Perkins, F. Fuller-Pace, and D. W. Meek. 2010. p53-dependent repression of polo-like kinase-1 (PLK1). *Cell Cycle* 9: 4200-4212.
168. Gjoerup, O. V., J. Wu, D. Chandler-Militello, G. L. Williams, J. Zhao, B. Schaffhausen, P. S. Jat, and T. M. Roberts. 2007. Surveillance mechanism linking Bub1 loss to the p53 pathway. *Proc Natl Acad Sci U S A* 104: 8334-8339.
169. Fischer, M. 2017. Census and evaluation of p53 target genes. *Oncogene* 36: 3943-3956.
170. Sbisa, E., D. Catalano, G. Grillo, F. Licciulli, A. Turi, S. Liuni, G. Pesole, A. De Grassi, M. F. Caratozzolo, A. M. D'Erchia, B. Navarro, A. Tullo, C. Saccone, and A. Gisel. 2007. p53FamTaG: a database resource of human p53, p63 and p73 direct target genes combining in silico prediction and microarray data. *BMC Bioinformatics* 8 Suppl 1: S20.
171. Li, Y., C. W. Jenkins, M. A. Nichols, and Y. Xiong. 1994. Cell cycle expression and p53 regulation of the cyclin-dependent kinase inhibitor p21. *Oncogene* 9: 2261-2268.
172. Zhang, Y., and H. Lu. 2009. Signaling to p53: ribosomal proteins find their way. *Cancer Cell* 16: 369-377.
173. Dai, M. S., and H. Lu. 2004. Inhibition of MDM2-mediated p53 ubiquitination and degradation by ribosomal protein L5. *J Biol Chem* 279: 44475-44482.
174. Yadavilli, S., L. D. Mayo, M. Higgins, S. Lain, V. Hegde, and W. A. Deutsch. 2009. Ribosomal protein S3: A multi-functional protein that interacts with both p53 and MDM2 through its KH domain. *DNA Repair (Amst)* 8: 1215-1224.
175. Laboratories, K. Cell cycle - Homo sapiens (human).
176. Zilfou, J. T., and S. W. Lowe. 2009. Tumor suppressive functions of p53. *Cold Spring Harb Perspect Biol* 1: a001883.
177. Choong, M. L., H. Yang, M. A. Lee, and D. P. Lane. 2009. Specific activation of the p53 pathway by low dose actinomycin D: a new route to p53 based cyclotherapy. *Cell Cycle* 8: 2810-2818.

178. Kukurba, K. R., and S. B. Montgomery. 2015. RNA Sequencing and Analysis. *Cold Spring Harb Protoc* 2015: 951-969.
179. Ando, K., T. Ozaki, H. Yamamoto, K. Furuya, M. Hosoda, S. Hayashi, M. Fukuzawa, and A. Nakagawara. 2004. Polo-like kinase 1 (Plk1) inhibits p53 function by physical interaction and phosphorylation. *J Biol Chem* 279: 25549-25561.
180. Sulic, S., L. Panic, M. Barkic, M. Mercep, M. Uzelac, and S. Volarevic. 2005. Inactivation of S6 ribosomal protein gene in T lymphocytes activates a p53-dependent checkpoint response. *Genes Dev* 19: 3070-3082.
181. Panic, L., S. Tamarut, M. Sticker-Jantscheff, M. Barkic, D. Solter, M. Uzelac, K. Grabusic, and S. Volarevic. 2006. Ribosomal protein S6 gene haploinsufficiency is associated with activation of a p53-dependent checkpoint during gastrulation. *Mol Cell Biol* 26: 8880-8891.
182. Chakraborty, A., T. Uechi, S. Higa, H. Torihara, and N. Kenmochi. 2009. Loss of ribosomal protein L11 affects zebrafish embryonic development through a p53-dependent apoptotic response. *PLoS One* 4: e4152.
183. Kuroda, J., Y. Kamitsuji, S. Kimura, E. Ashihara, E. Kawata, Y. Nakagawa, M. Takeuichi, Y. Murotani, A. Yokota, R. Tanaka, M. Andreeff, M. Taniwaki, and T. Maekawa. 2008. Anti-myeloma effect of homoharringtonine with concomitant targeting of the myeloma-promoting molecules, Mcl-1, XIAP, and beta-catenin. *Int J Hematol* 87: 507-515.
184. Collin, R., C. St-Pierre, L. Guilbault, V. Mullins-Dansereau, A. Policheni, F. Guimont-Desrochers, A. N. Pelletier, D. H. Gray, E. Drobetsky, C. Perreault, E. E. Hillhouse, and S. Lesage. 2017. An Unbiased Linkage Approach Reveals That the p53 Pathway Is Coupled to NK Cell Maturation. *J Immunol* 199: 1490-1504.
185. Pelletier, A. N., L. Guilbault, F. Guimont-Desrochers, E. E. Hillhouse, and S. Lesage. 2016. NK Cell Proportion and Number Are Influenced by Genetic Loci on Chromosomes 8, 9, and 17. *J Immunol* 196: 2627-2636.

Appendix

Table A1: Flow cytometry antibodies

Marker	Color	Dilution	Clone	Company	Catalogue #
CD3	APC-780	1:200	17A2	eBioscience	47-0032-82
NK1.1	FITC	1:150	PK136	eBioscience	11-5941-85
CD27	PE-Cy7	1:100	LG.3A10	Biolegend	124215
CD11b	EF-450	1:300	M1/70	invitrogen	48-0112-82
KLRG1	PE	1:200	2F1	eBioscence	12-5893-82
NK1.1	PE	1:150	PK136	eBioscience	12-5941-83
NKp46	EF-450	1:150	29A1.4	invitrogen	48-3351-82
Ly49H	APC	1:200	3D10	eBioscience	17-5886-82
Ly49G2	PerCP 710	1:200	4D11	eBioscience	46-5781-82
CD122	FITC	1:200	TM-b1	invitrogen	11-1222-82

Table A2: Cell sorting antibody panel

Marker	Color	Dilution	Clone	Company	Catalogue #
NK1.1	PE	1:150	PK136	eBioscience	12-5941-83
NKp46	PerCP 710	1:150	29A1.4	eBioscience	46-3351-82
CD49b	FITC	1:150	DX5	Biolegend	108906
CD3	APC	1:200	17A2	eBioscience	17-0032-82
CD19	APC	1:300	1D3	eBioscience	17-0193-80

Table A3: NK cell purity and RNA quality

Sample	Sex	Age	Total lymphocyte #	NK cell #	% purity	RIN score	Total ng RNA
Gnl1$^{+/+}$ 1	Male	10.86	94 x 10^6	6.25 x 10^5	87.1	8.8	191
Gnl1$^{+/+}$ 2	Male	8.43	73.5 x 10^6	5.18 x 10^5	87.8	8.9	46.6
Gnl1$^{+/+}$ 3	Male	8.29	115.5 x 10^6	5.18 x 10^5	91.1	9.0	78.5
Gnl1^{C365X} 1	Male	7.43	38 x 10^6	1.07 x 10^5	77.9	9.3	22.3
Gnl1^{C365X} 2	Male	7.86	57.7 x 10^6	1.41 x 10^5	88.8	9.4	15.3
Gnl1^{C365X} 3	Male	7.71	55.6 x 10^6	1.77 x 10^5	85.9	9.5	19.2

Table A4: RNA-sequencing set-up and quality control

Sample	Run-type	Library Type	Type of Sequencing	Raw paired end reads #	Average Quality	% Duplicates
Gnl1$^{+/+}$ 1				62,900,352		59.4
Gnl1$^{+/+}$ 2	Paired	rRNA	Illumina	47,005,859	38	47.501
Gnl1$^{+/+}$ 3	end 50	depleted	HiSeq 4000	54,226,719		45.887
Gnl1^{C365X} 1				49,350,943		48.616
Gnl1^{C365X} 2				59,680,954		50.182
Gnl1^{C365X} 3				50,013,813		42.84

Table A5: Sequencing alignment results

Sample	Raw PE reads #	Surviving PE reads # (trimming)	% Surviving	Mapped PE reads	% aligned	Exonic rate
Gnl1$^{+/+}$ 1	62,900,352	58,914,533	93.7	34,392,525	55.0	0.698
Gnl1$^{+/+}$ 2	47,005,859	43,902,148	93.4	30,196,832	68.8	0.750
Gnl1$^{+/+}$ 3	54,227,219	52,989,810	97.7	37,395,778	70.6	0.779
Gnl1^{C365X} 1	49,350,943	47,735,509	96.7	31,209,087	65.4	0.689
Gnl1^{C365X} 2	59,680,954	54,106,085	90.7	38,421,277	71.0	0.780
Gnl1^{C365X} 3	50,001,813	48,125,291	96.2	35,468,277	73.7	0.786

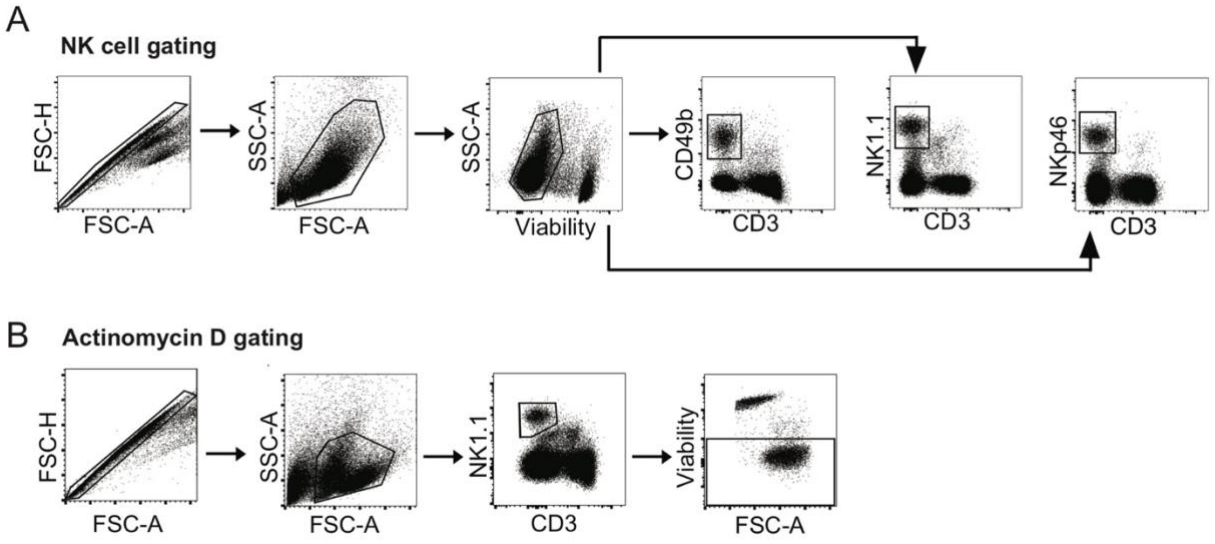

Figure A1: Flow cytometry gating strategies
Flow cytometry gating strategy for identification of **(A)** NK cells or **(B)** in the actinomycin D experiment. **(A)** Singlets (FSC-A by FSC-H), Lymphocytes (FSC-A by SSC-A), Viability (Viability by SSC-A), NK cells ($CD49b^{+}CD3^{-}$) or ($NK1.1^{+}CD3^{-}$) or ($NKp46^{+}CD3^{-}$). **(B)** Singlets (FSC-A by FSC-H), Singlets (FSC-A by SSC-A), NK cells ($NK1.1^{+}CD3^{-}$) and Viability (FSC-A by Viability).

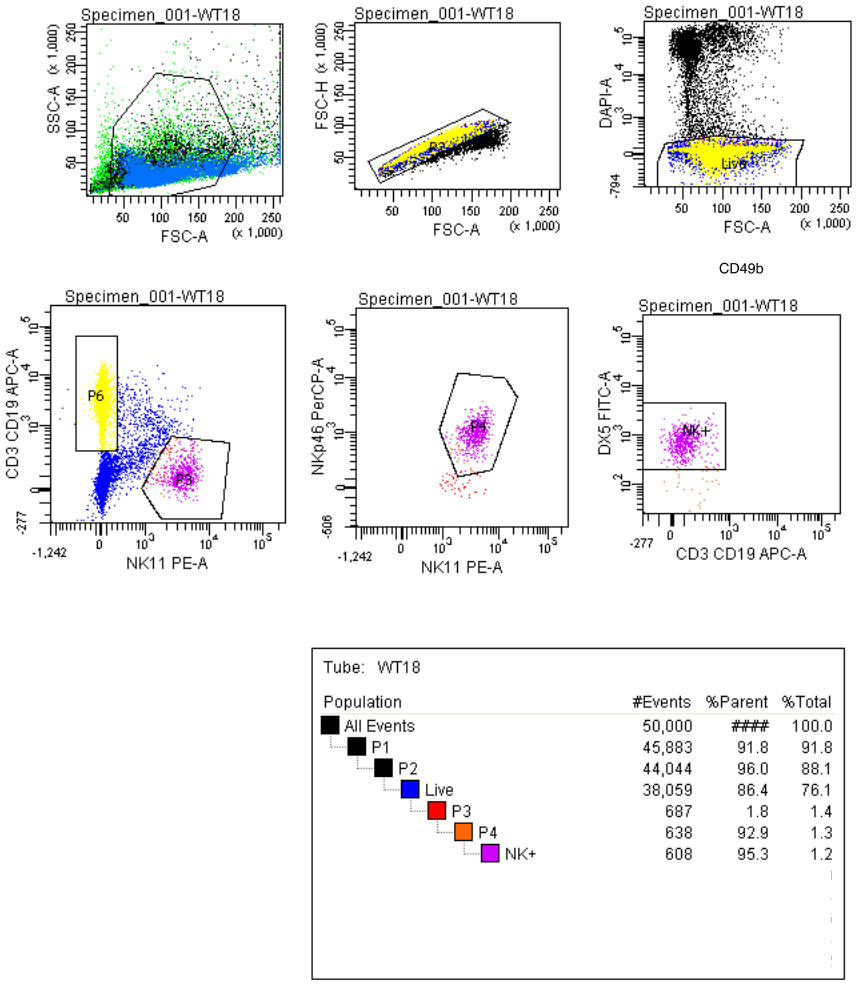

Tube: WT18

Population	#Events	%Parent	%Total
All Events	50,000	####	100.0
P1	45,883	91.8	91.8
P2	44,044	96.0	88.1
Live	38,059	86.4	76.1
P3	687	1.8	1.4
P4	638	92.9	1.3
NK+	608	95.3	1.2

Figure A2: NK cell sorting gating strategy
NK cell gating strategy used to sort *Gnl1*$^{+/+}$ and *Gnl1*^{C365X} splenic NK cells. Gating strategy used to sort pure NK cells; Lymphocytes (FSC-A by SSC-A), Singlets (FSC-A by FSC-H), Live cells (FSC-A by DAPI^{-}), NK cells [(NK1.1^{+}CD3^{-}CD19^{-}), (NK1.1^{+}NKp46^{+}) and (CD3^{-}CD19^{-}DX5^{+})].